IPCC Chapter 5: **Informations from paleoclimate archives**

- Introduction *(Section 5.1)*
- Pre-industrial perspective on radiative forcing factors *(Section 5.2)*
- Earth System Responses and Feedbacks *(Section 5.3)*
- Executive summary *(Ch. 5)*

Masson-Delmotte, V., et al., 2013: Information from Paleoclimate Archives. In: Climate Change 2013: The Physical Science Basis. Contribution of Working Group I to the Fifth Assessment Report of the Intergovernmental Panel on Climate Change. Cambridge University Press.

Chapter 5 - Topic presentations

- Volcanic Eruptions and Climate – cause for the litte Ice Age? Malte

- Polar amplification in the past (IPCC chapter 5, updated papers) Christine

Q: Why is stronger pH decrease over the Arctic?

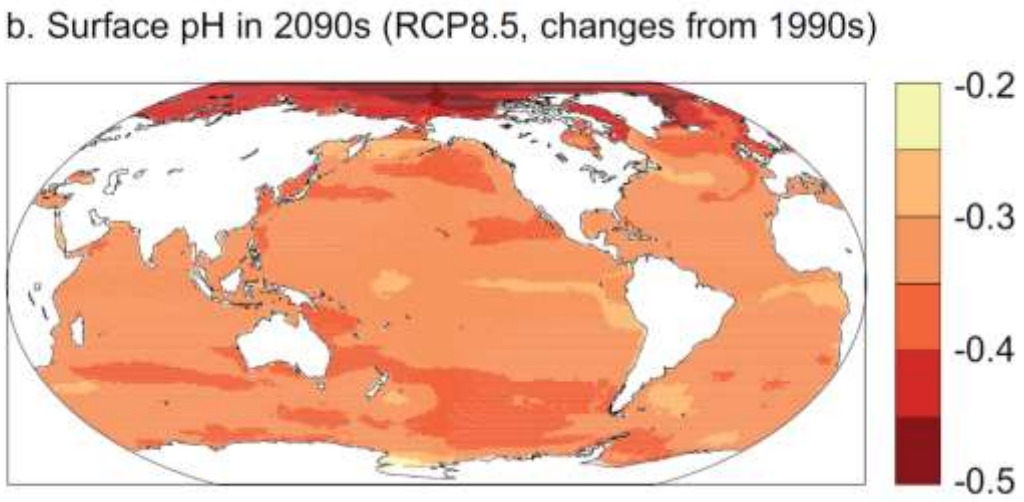

"An exception is the Arctic Ocean where reductions in pH and CaCO3 saturation states are projected to be exacerbated by effects from **increased freshwater input due to sea ice melt**, **more precipitation, and greater air–sea CO2 fluxes due to less sea ice cover** (Steinacher et al., 2009; Yamamoto et al., 2012)."

Background Informations

-Proxies

-Reconstructions

-Models

Can we quantify past climate change?

high resolution climate archives with annual layering

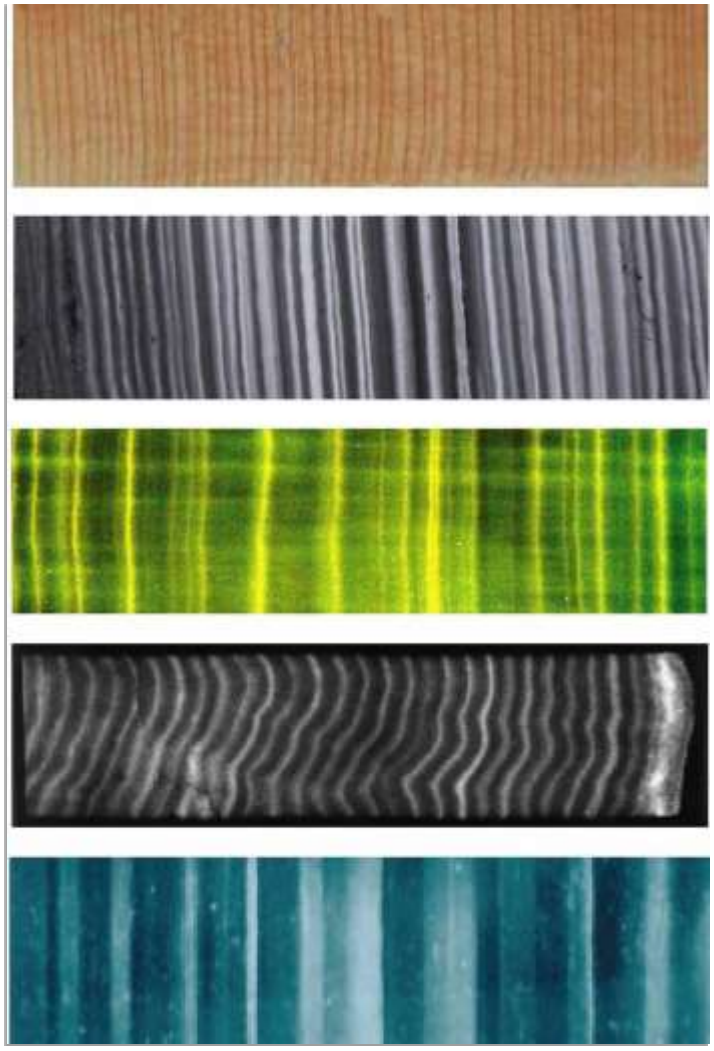

Tree rings

Lake sediments

Speleothems

Corals

Ice cores

Cooler climate reduces tree growth, causing thinner tree rings (frost rings).

Ice Cores as Climate Archives

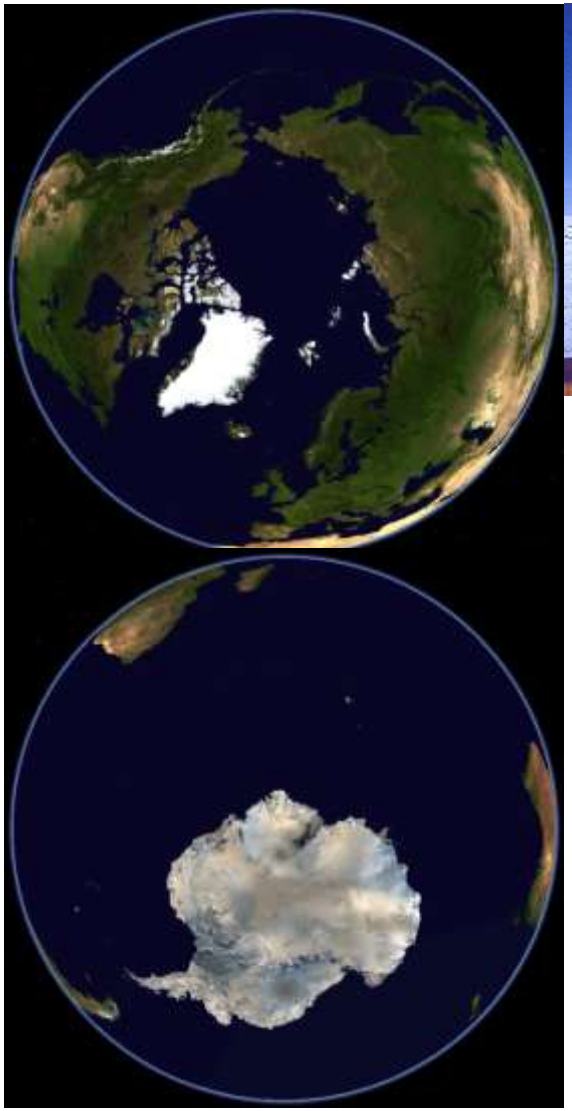

young

old

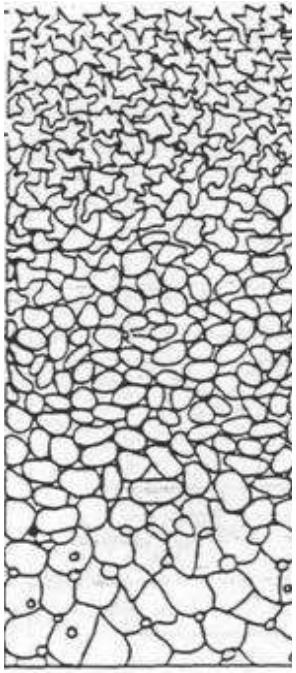

snow

firn

ice

Marine sediment cores as climate archives

up to 180 Mio years back in time

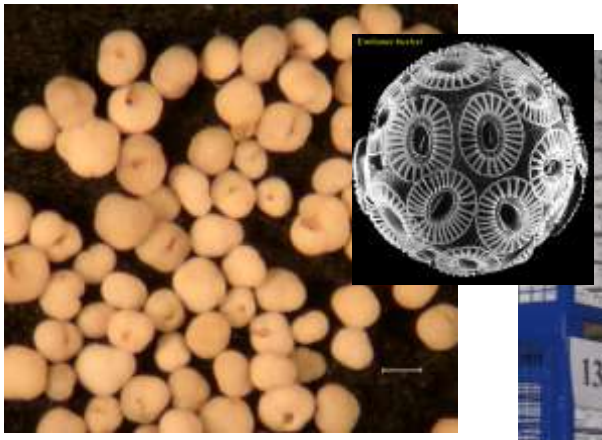

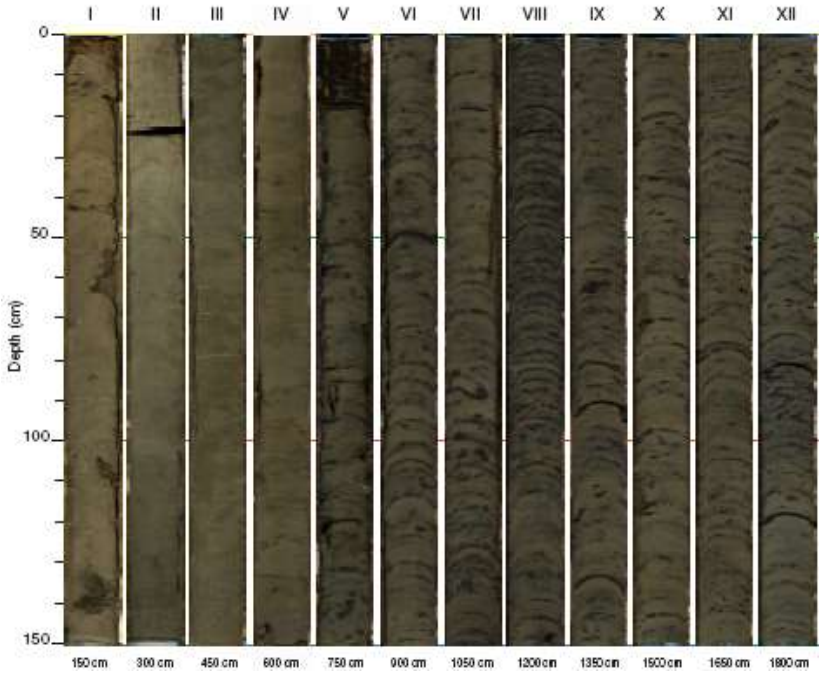

Core Lab Work

cut **split** **label** **log** **describe**

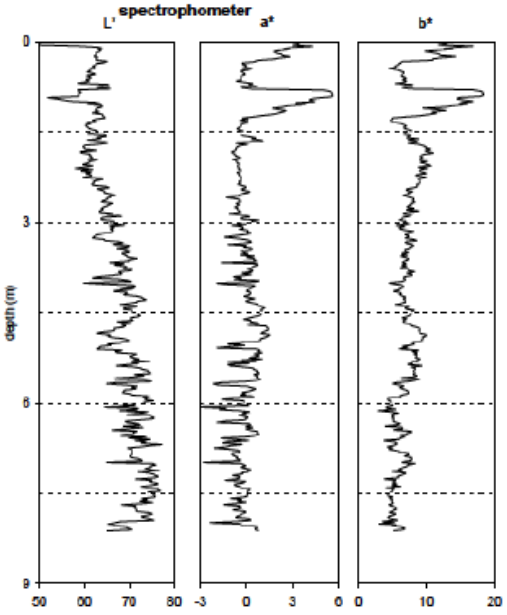

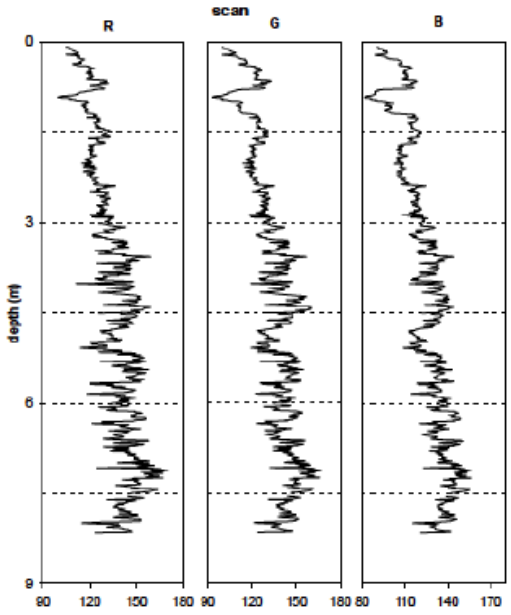

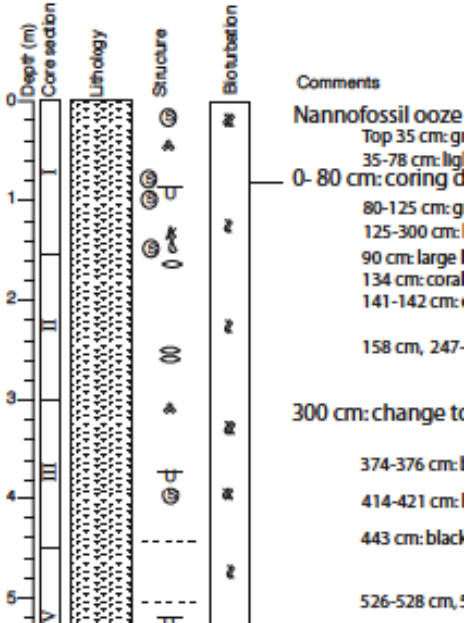

Climate archives

Source	Time (years)	Climate variable
1. Instruments	250	temperature, pressure, wind, precipitation
2. Historical documents floods, strong winters, crop failure, wine quality, corn prices, coastal ice, etc.	1000	temperature, precipitation
3. Paleoclimate data		
tree rings	10000	temperature, precipitation
varves	10000	temperature, precipitation
ice cores ($d^{18}O$)	100000	temperature
pollen	100000	temperature, precipitation
marine sediments	1000000	
fauna		temperature, sea-ice coverage
$d^{18}O$		continental ice volume
dust (grain size)		wind speed and direction

Isotopes

CO_2 proxies

Marine proxies from ocean sediments:
-Alkenone (phyto- plankton marker)
-Boron isotopes in foraminifera

Terrestrial proxies from soil (paleosols) and fossils:
-Carbon isotopes in soil carbonate and organic matter
-Stomata in fossil plant leaves
-Nahcolite (baking soda) a mineral
-Liverwort (plant)

Table 5.A.2 | Summary of atmospheric carbon dioxide (CO_2) proxy methods and confidence assessment of their main assumptions.

Method	Scientific Rationale	Estimated Applicability	Limitations	Main Assumptions (relative confidence)
Alkenone (phytoplankton biomarker) carbon isotopes	Measurements of carbon isotope ratios of marine sedimentary alkenones (or other organic compounds) allows determination of the isotopic fractionation factor during carbon fixation (ε_p) from which pCO_2 can be calculated.	100 to ~4000 ppm; 0 to 100 Ma	Alkenones are often rare in oligotrophic areas and sometimes absent. Method relies on empirical calibration and $\delta^{13}C$ is sensitive to other environmental factors, especially nutrient-related variables. Method has been used successfully to reconstruct glacial–interglacial changes.	Measured alkenone carbon isotope ratio is accurate and precise (*high*). Ambient aqueous partial pressure of carbon dioxide (pCO_2) has a quantifiable relationship with ε_p that can be distinguished from the nutrient-related physiological factors such as algal growth rate, cell size, cell geometry and light-limited growth (*medium*). Aqueous pCO_2 is in equilibrium with atmospheric pCO_2 (*medium*). Carbon isotope fractionation in modern alkenone-producing species is the same in ancient species and constant through time (*medium*). Levels of biological productivity (e.g., dissolved phosphate concentrations) can be calculated (*high*). Carbon isotope ratio of aqueous CO_2 in the mixed layer can be determined (*medium*). Sea surface temperature can be determined (*high*). Atmospheric partial pressure of oxygen (pO_2) is known or assumed (*medium*). Diagenetic effects are minimal, or can be quantified (*medium*).
Boron isotopes in foraminifera	Boron isotope ratios ($\delta^{11}B$) in foraminifera (or other calcifying organisms) give paleo-pH from which pCO_2 can be calculated if a value for a second carbonate system parameter (e.g., alkalinity) is assumed.	100 to ~4000 ppm; 0 to 100 Ma	Calculated pCO_2 is very sensitive to the boron isotope ratio of seawater which is relatively poorly known, especially for the earlier Cenozoic. Effects of foraminiferal preservation are not well understood. Method has been used successfully to reconstruct glacial–interglacial changes.	Measured boron isotope ratio is accurate and precise (*high*). The equilibrium constant for dissociation of boric acid and boron isotopic fractionation between $B(OH)_3$ and $B(OH)_4^-$ are well known (*high*). Boron incorporation into carbonate is predominantly from borate ion (*high*). Boron isotope ratio of foraminifer calcification reflects ambient surface seawater pH (*high*). Aqueous pCO_2 is in equilibrium with atmospheric pCO_2 (*medium*). Habitats of extinct species can be determined (*high*). There is no vital effect fractionation in extinct species, or it can be determined (*medium*). The boron isotope ratio of seawater ($\delta^{11}B_{sw}$) can be determined (*medium*). Ocean alkalinity or concentration of Total Dissolved Inorganic Carbon can be determined (*high*). Sea surface temperature (SST) and salinity (SSS) can be determined (*high*). Diagenetic effects are minimal or can be quantified (*high*).
Carbon isotopes in soil carbonate and organic matter	Atmospheric pCO_2 affects the relationship between the $\delta^{13}C$ of soil CO_2 and the $\delta^{13}C$ of soil organic matter at depth in certain soil types, hence measurement of these parameters in paleosols can be used to calculate past pCO_2.	1000 to ~4000 ppm; 0 to 400 Ma	Method works better for some soil types than others. CO_2 loss is difficult to quantify and method and effects of late diagenesis may be difficult to determine.	Isotopic composition of soil CO_2 is reflected in soil carbonates below a depth of 50 cm. (*medium*). The concentration of respired CO_2 in the soil is known or assumed (*medium*). Isotopic composition of atmospheric CO_2 is known or can be inferred (*low*). Soil carbonates were precipitated in the vadose zone in exchange with atmospheric CO_2 (*high*). The original depth profile of a paleosoil can be determined (*low*). Burial (late) diagenetic effects are minimal or can be quantified (*high*).
Stomata in plant leaves	The relative frequency of stomata on fossil leaves (Stomatal Index; (Salisbury, 1928) can be used to calculate past atmospheric CO_2 levels.	100 to ~1000 ppm; 0 to 400 Ma	Closely related species have very different responses to pCO_2. The assumption that short-term response is the same as the evolutionary response is difficult to test. This and the shape of the calibration curves mean that much greater certainty applies to low pCO_2 and short time scales.	Measured stomatal index is accurate and precise (*high*). Measured stomatal index is representative of the plant (*high*). The target plants adjust their stomatal index of leaves to optimize CO_2 uptake (*medium*). Atmospheric pCO_2 close to the plant is representative of the atmosphere as a whole (*medium*). The quantitative relationship between stomatal index and CO_2 observed on short time scales (ecophenotypic or 'plastic response') applies over evolutionary time (*low*). Environmental factors such as irradiance, atmospheric moisture, water availability, temperature, and nutrient availability do not affect the relationship between stomatal index and CO_2 (*medium*). Stomatal index response to CO_2 of extinct species can be determined or assumed (*low*). Taphonomic processes do not affect stomatal index counts (*high*). Diagenetic processes do not affect stomatal index counts (*high*).

Temp recon-structions:

Based on proxy data:
-Tree rings
-Ice cores
-Lake and ocean sediments
-Glacier records
-Boreholes
-Pollens
-Corals

Table 5.A.6 | Hemispheric and global temperature reconstructions assessed in Table 5.4 and used in Figures 5.7 to 5.9.

Reference [Identifier]	Period (CE)	Resolution	Region[a]	Proxy Coverage[b]				Method & Data
				H	M	L	O	
Briffa et al. (2001) [only used in Figure 5.8b–d due to divergence issue]	1402–1960	Annual (summer)	L 20°N to 90°N	✱	☒	☐	☐	Principal component forward regression of regional composite averages. Tree-ring density network, age effect removed via age-band decomposition.
Christiansen and Ljungqvist (2012) [CL12loc]	1–1973	Annual	L+S 30°N to 90°N	✱	✱	☐	☐	Composite average of local records calibrated by local inverse regression. Multi-proxy network.
D'Arrigo et al. (2006) [Da06treecps]	713–1995	Annual	L 20°N to 90°N	✱	☒	☐	☐	Forward linear regression of composite average. Network of long tree-ring width chronologies, age effect removed by Regional Curve Standardisation.
Frank et al. (2007) [Fr07treecps]	831–1992	Annual	L 20°N to 90°N	☒	☒	☐	☐	Variance matching of composite average, adjusted for artificial changes in variance. Network of long tree-ring width chronologies, age effect removed by Regional Curve Standardisation.
Hegerl et al. (2007) [He07tls]	558–1960	Decadal	L 30°N to 90°N	☒	☒	☐	☐	Total Least Squares regression. Multi-proxy network.
Juckes et al. (2007) [Ju07cvm]	1000–1980	Annual	L+S 0° to 90°N	☒	☒	☐	☐	Variance matching of composite average. Multi-proxy network.
Leclercq and Oerlemans (2012) [LO12glac]	1600–2000	Multidecadal	L 0° to 90°N L 90S to 0° L 90°S to 90°N	☒	✱	☒	☐	Inversion of glacier length response model. 308 glacier records.
Ljungqvist (2010) [Lj10cps]	1–1999	Decadal	L+S 30°N to 90°N	✱	☒	☐	☒	Variance matching of composite average. Multi-proxy network.
Loehle and McCulloch (2008) [LM08ave]	16–1935	Multidecadal	L+S mostly 0° to 90°N	☒	☒	☐	☒	Average of calibrated local records. Multi-proxy network (almost no tree-rings).
Mann et al. (2008) [Ma08cpsl] [Ma08eivl] [Ma08eivf] [Ma08min7eivf]	200–1980	Decadal	L [cpsl/eivl] and L+S [eivf] versions, 0° to 90°N, 0° to 90°S, and 90°S to 90°N	✱	✱	☒	☒	(i) Variance matching of composite average. (ii) Total Least Squares regression. Multi-proxy network.[c]
Mann et al. (2009) [Ma09regm]	500–1849	Decadal	L+S 0 to 90°N	✱	✱	☒	☒	Regularized Expectation Maximization with Truncated Total Least Squares. Multi-proxy network.[c]
Moberg et al. (2005) [Mo05wave]	1–1979	Annual	L+S 0° to 90°N	☒	✱	☒	☐	Variance matching of composites of wavelet decomposed records. Tree-ring width network for short time scales; non-tree-ring network for long time scales.
Pollack and Smerdon (2004) [PS04bore]	1500–2000	Centennial	L 0° to 90°N L 0° to 90°S L 90°S to 90°N	☒	✱	☒	☐	Borehole temperature profiles inversion
Shi et al. (2013) [Sh13pcar]	1000–1998	Annual	L 0 to 90°N	✱	☒	☐	☐	Principal component regression with autoregressive timeseries model. Multi-proxy network (tree-ring and non-tree-ring versions).

Notes:
[a] Region: L = land only, L+S = land and sea, latitude range indicated.
[b] Proxy location and coverage: H = high latitude, M = mid latitude, L = low latitude, O = oceans, ☐ = none or very few, ☒ = limited, ✱ = moderate
[c] These studies also present versions without tree-rings or without seven inhomogeneous proxies (including the Lake Korttajärvi sediment records; Tiljander et al., 2003). The latter version is used in Figure 5.7a (Ma08min7eivf) in preference to the reconstruction from the full network. The impact of these seven proxies on the other NH reconstructions is negligible (MA08cpsl) or results in a slightly warmer pre-900 reconstruction compared to the version without them (Ma09regm).

Model data:

-**AOGCM**:
Atmosphere Ocean Generel Circulation Model

-**ESM**:
Earth System Model

Model	(No. runs) Period	Forcings[a]	Reference
Pre PMIP3/CMIP5 Experiments			
CCSM3	(1×) 1000–2000 (4×) 1500–2000	SS^{11}·V^{22}·$G^{30,31,35}$	Hofer et al. (2011)
CNRM-CM3.3	(1×) 1001–1999	SS^{17}·V^{21}·$G^{30,34,35}$·A^{44}·L^{54}	Swingedouw et al. (2011)
CSM1.4	(1×) 850–1999	SS^{10}·V^{21}·$G^{30,31,35}$·A^{41}	Ammann et al. (2007)
CSIRO-MK3L-1-2	(3×) 1–2001 (3×) 1–2001 (3×) 501–2001	SW^{14} SW^{14}·G^{34}·O^{60} SW^{14}·V^{24}·G^{34}·O^{60}	Phipps et al. (2013)
ECHAM4/OPYC	(1×) 1500–2000	SS^{11}·$V^{21,26}$·G^{38}·A^{42}·L^{55}	Stendel et al. (2006)
ECHAM5/MPIOM	(5×) 800–2005 (3×) 800–2005	SW^{13}·V^{25}·$G^{34,39}$·A^{40}·L^{53}·O^{61} SS^{10}·V^{25}·$G^{34,39}$·A^{40}·L^{53}·O^{61}	Jungclaus et al. (2010)
ECHO-G	(1×) 1000–1990 (1×) 1000–1990 (2×) –7000–1998	SS^{11}·V^{20}·$G^{31,36,37}$ SS^{11}·V^{20}·$G^{31,36,37}$ SS^{12}·G^{30}·O^{62}	González-Rouco et al. (2003)[b] González-Rouco et al. (2006) Wagner et al. (2007)
HadCM3	(1×) 1492–1999	SS^{17}·V^{23}·G^{32}·A^{43}·$L^{50,54,55}$·O^{60}	Tett et al. (2007)
IPSLCM4	(1×) 1001–2000	SS^{11}·$G^{30,34,35}$·A^{44}·O^{63}	Servonnat et al. (2010)
FGOALS-gl	(1×) 1000–1999	SS^{11}·V^{20}·$G^{30,31,35}$	Zhou et al. (2011)[c]
PMIP3/CMIP5 Experiments			
BCC-csm1-1	(1×) 850–2005	SW^{15}·V^{24}·$G^{30,33,34}$·A^{45}·O^{60}	
CCSM4	(1×) 850–2004	SW^{15}·V^{24}·$G^{30,33,34}$·A^{45}·L^{51}·O^{60}	Landrum et al. (2013)
CSIRO-MK3L-1-2	(1×) 851–2000	SW^{14}·V^{25}·$G^{30,33,34}$·O^{60}	
GISS-E2-R	(8×) 850–2004	SW^{14}·V^{25}·$G^{30,33,34}$·A^{45}·L^{51}·O^{60} SW^{14}·V^{24}·$G^{30,33,34}$·A^{45}·L^{51}·O^{60} SW^{14}·$G^{30,33,34}$·A^{4}·L^{51}·O^{60} SW^{15}·V^{25}·$G^{30,33,34}$·A^{45}·L^{51}·O^{60} SW^{15}·V^{24}·$G^{30,33,34}$·A^{45}·L^{52}·O^{60} SW^{15}·$G^{30,33,34}$·A^{4}·L^{51}·O^{60} SW^{15}·V^{25}·$G^{30,33,34}$·A^{45}·L^{52}·O^{60} SW^{15}·V^{24}·$G^{30,33,34}$·A^{45}·L^{51}·O^{60}	[d]
HadCM3	(1×) 800–2000	SW^{14}·V^{25}·$G^{30,32,34}$·A^{43}·L^{51}·O^{60}	Schurer et al. (2013)
IPSL-CM5A-LR	(1×) 850–2005	SW^{15}·V^{27}·$G^{30,33,34}$·O^{60}	
MIROC-ESM	(1×) 850–2005	SW^{16}·V^{25}·$G^{30,34,39}$·O^{60}	[e]
MPI-ESM-P	(1×) 850–2005	SW^{15}·V^{25}·$G^{30,33,34}$·A^{45}·L^{51}·O^{60}	

Simulations in red were excluded from Figs 5.8, 5.9 and 5.12

Climate models

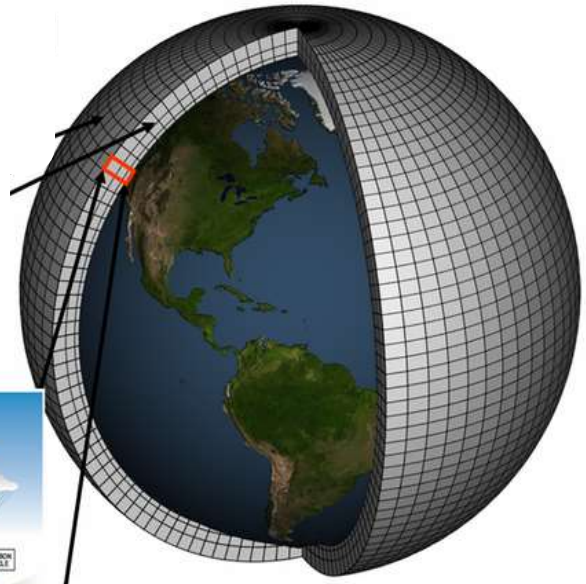

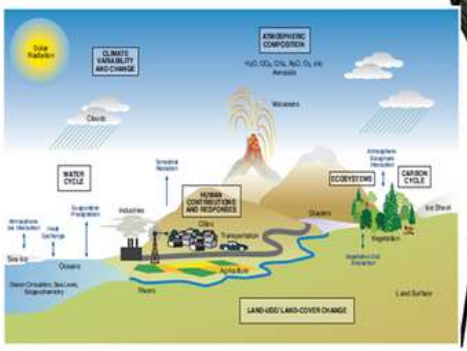

NOAA

- Background
- Types
- Development
- Spatial resolution
- Model runs and experiments
- Model forcing and response

What is an atmospheric model?

- An **atmospheric model** is a physical model solving the **primitive dynamical equations** to simulate atmospheric motions.
- It can supplement these equations with **parameterizations*** for turbulent diffusion, radiation, moist processes (clouds and precipitation), convection, gravity waves etc.
- Atmospheric models are solved **numerically**, i.e. they discretize equations of motion.
- It can **predict microscale, sub-microscale, as well as synoptic and global flows**.
- The horizontal domain of a model is either ***global***, covering the entire Earth, or ***regional*** covering only parts of the Earth.

*Parameterization refers to a method of replacing processes that are too small-scale or complex to be physically resolved in the model.

What type of numerical models exists?

Weather predictions:

Numerical Weather Prediction (NWP) models: global and regional models

Climate projections:

- **General Circulation Model** (GCM):
  - Atmosphere GCM (AGCM)
  - Ocean GCM (OGCM)
- **Climate models**:
  - **AOGCM**
  - **CMIP3** models: Climate Model Intercomparison Project 3 for IPCC AR4 (most were low top models with model lid @10 hPa)
  - **CMIP5** models: IPCC AR5 (low and high top models (model lid >60 km r >0.1hPa)
  - **PMIP3** models**:** Paleo Model Intercomparison Project models for IPCC AR4

What types of numerical models exist?

Earth System studies:

- **ESM**: Earth System Models
  - Complex fully coupled atmosphere ocean/sea ice, carbon cycle, biogeochemistry, vegetation models; also with full atmospheric chemistry and land ice
  - partly used in CMIP5

- **EMIC**: Earth System Model of Intermediate Complexity
  - Limited physical processes included
  - 2D or 3D
  - Long transient runs

Paleo climate studies:

- **PMIP**: Paleo Model Intercomparison Project models:
  - coupled climate models (low top AOGCMs)
  - limited spatial resolution enables long transient runs
- **EMIC**: as above

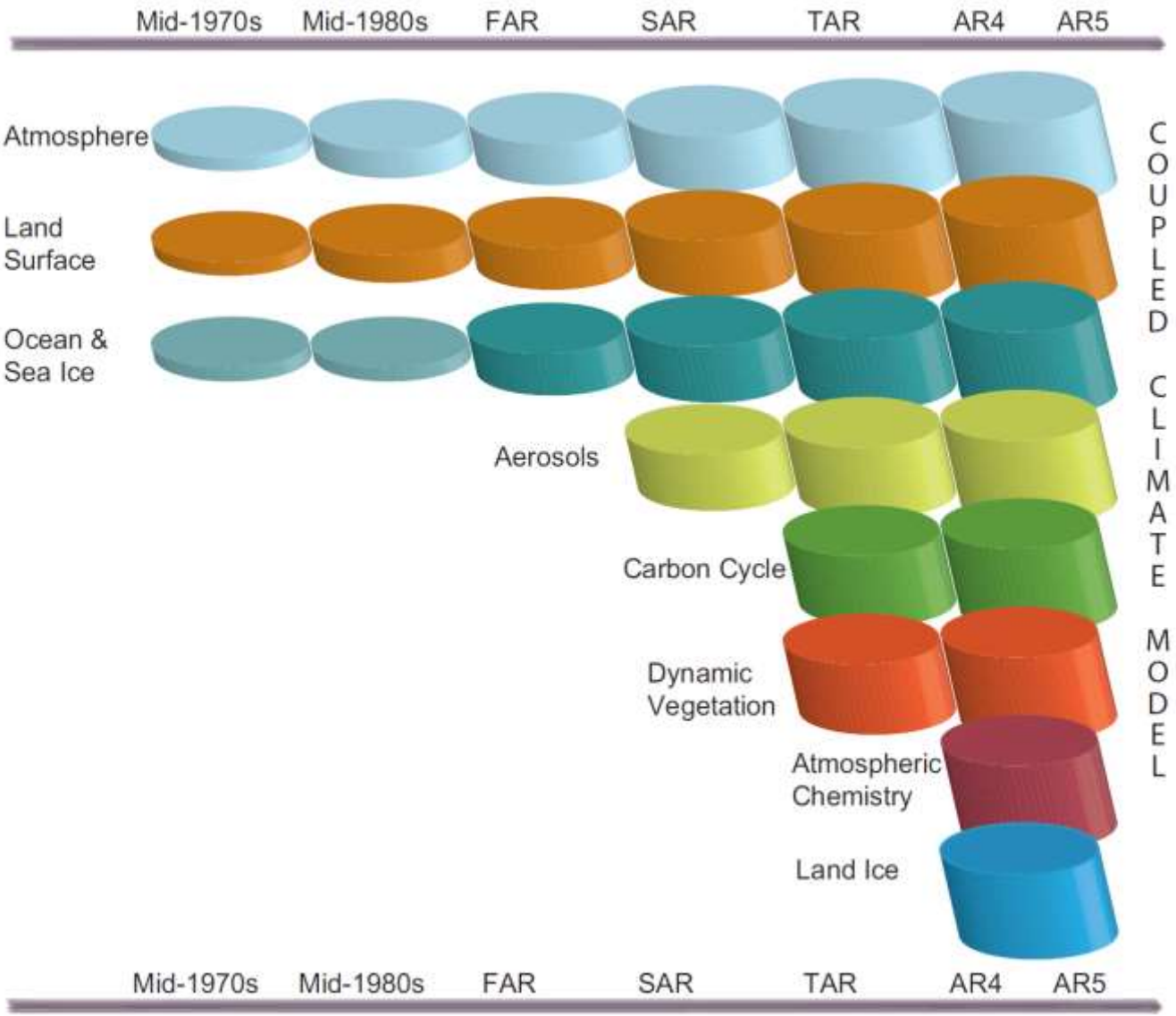

Figure 1.13 | The development of climate models over the last 35 years showing how the different components were coupled into comprehensive climate models over time. In each aspect (e.g., the atmosphere, which comprises a wide range of atmospheric processes) the complexity and range of processes has increased over time (illustrated by growing cylinders). Note that during the same time the horizontal and vertical resolution has increased considerably e.g., for spectral models from T21L9 (roughly 500 km horizontal resolution and 9 vertical levels) in the 1970s to T95L95 (roughly 100 km horizontal resolution and 95 vertical levels) at present, and that now ensembles with at least three independent experiments can be considered as standard.

Ch. 1 IPCC, 2013

Spatial model resolution

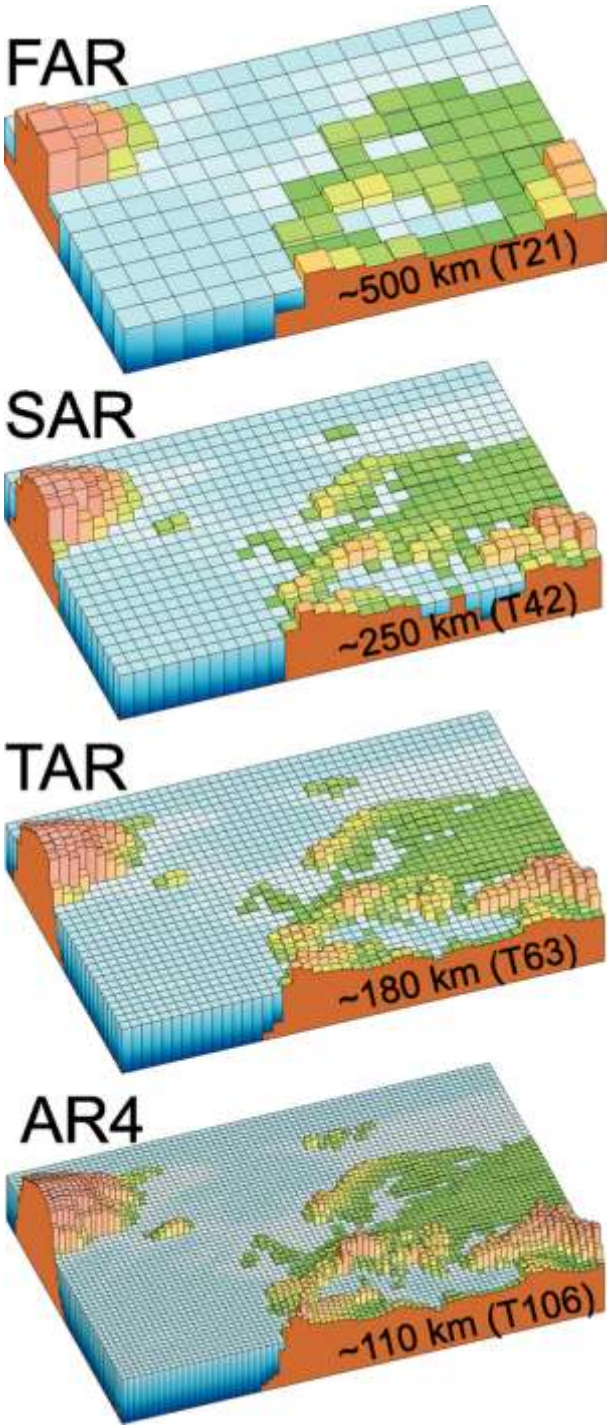

Ch. 1 IPCC, 2007

Model runs and model experiments

Model runs:

- Control run (CTR): e.g. present-day climatology
- Experiment (EXP):
  - Transient runs (historical runs, RCP future runs, hindcast runs)
  - Time slice runs (e.g. 2000 state runs)
  - Perpetual runs (e.g. perpetual January runs)

Model experiment: *a scientific question or model experiment should be anwsered by implementing a model forcing to the model*

- What is the effect of Arctic sea ice loss?
- What is the effect of greenhouse gas increase?
- What is the effect of ENSO on the atmosphere?

Model forcing – model response

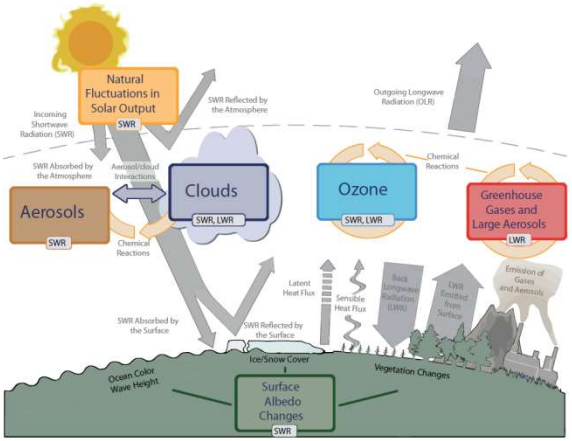

- For a model experiment a **forcing** is prescribed:
  e.g. RCP8.5 scenario, volcanic and solar forcing, Arctic sea ice loss…
- Radiative forcing (IPCC Chapter 8):
  resulting radiative response to implemented model forcing

- **Radiative (model) response**
  -ΔRad= Rad(EXP)-Rad(CTR)
- **Climate (model) response**
  -e.g. ΔSAT=SAT(EXP)-SAT(CTR)
  -e.g. ΔSST= SST(El Nino yrs)-SST(no ENSO yrs)

Main drivers of climate change

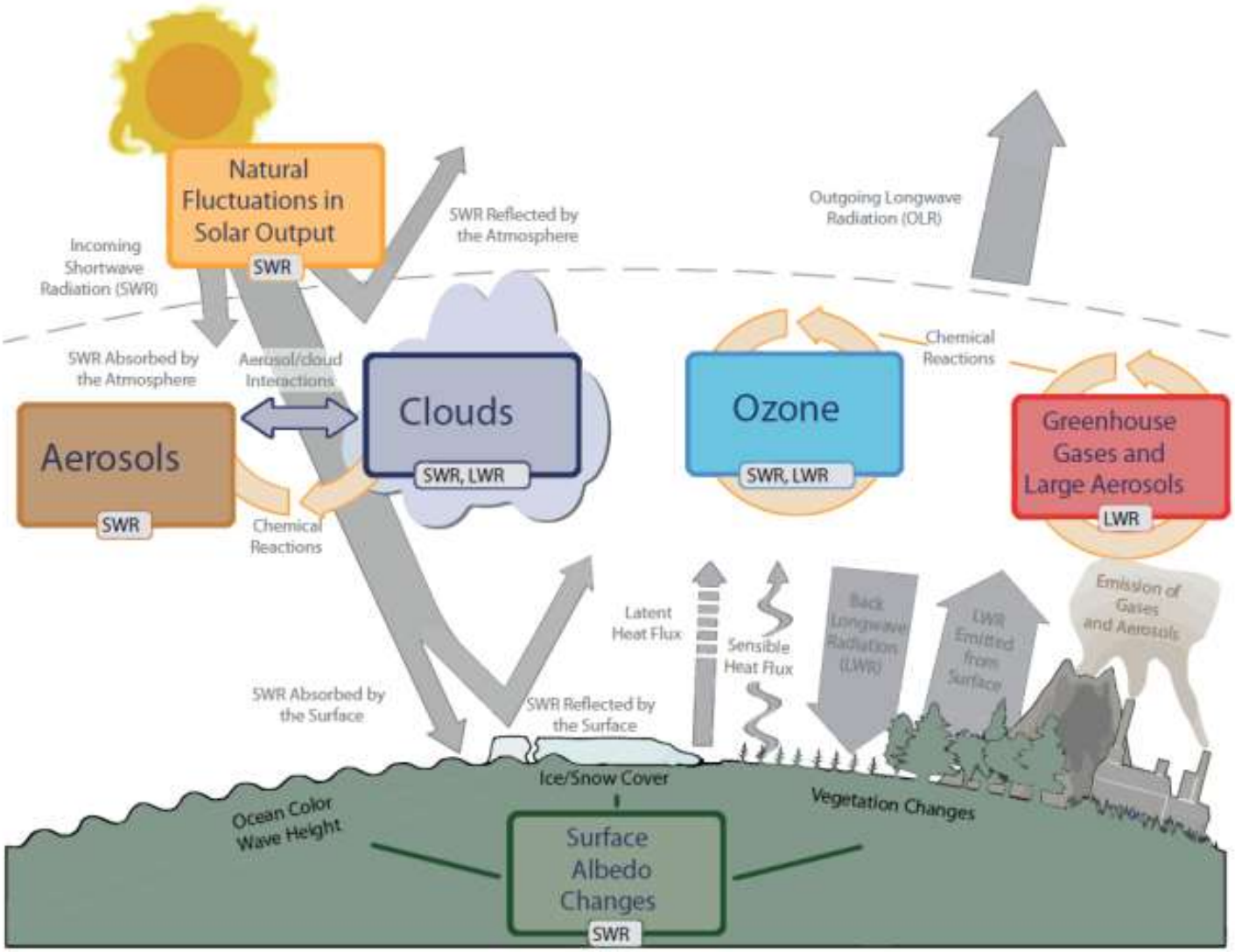

Chapter 1 IPCC (2013)

Pre-industrial perspective on radiative forcing factors *(Section 5.2)*

Radiative forcing factors

External forcing:

- Volcanic Forcing
- Solar Forcing
- Orbital Forcing

Greenhouse gases, aerosols, and dust:

- CO_2, CH_4, N_2O, dust and aerosols

Last Millennium 1 ka- Reconstructed Volcanic forcing

based on ice core records

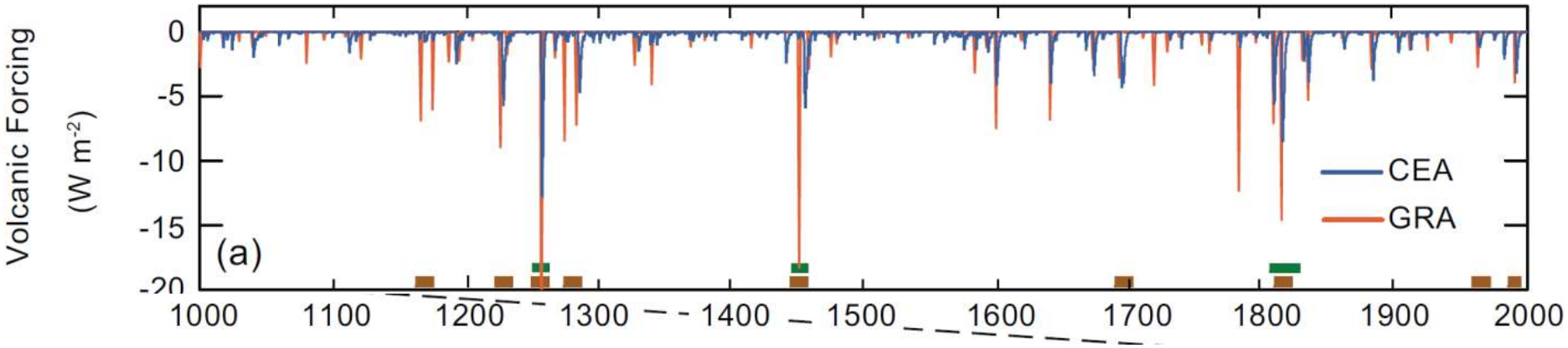

Stratospheric origin: Greenland, Antarctica

–Crowley and Unterman (2013)

–GRA: Gao, Robock and Ammann (2008 & 2012)

Pinatubo AOD used in CMIP5 models

AOD: Gao

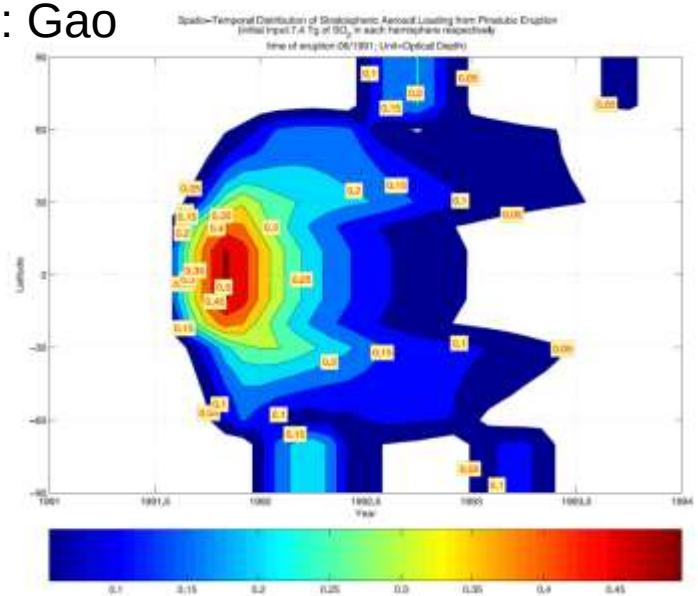

Crowley and Untermann (2013 volcanic forcing has only 4 bands of AOD(0.5um) and Reff: 90-30N, 30-0N,0-30S, 30-90S

AOD: Sato

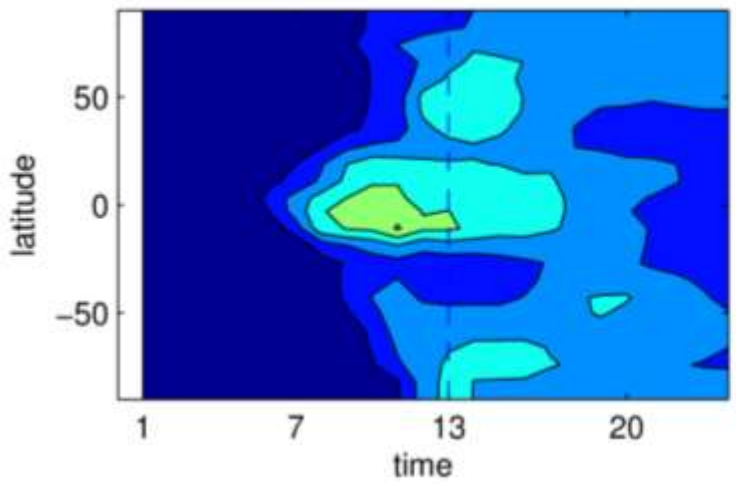

AOD: Ammann

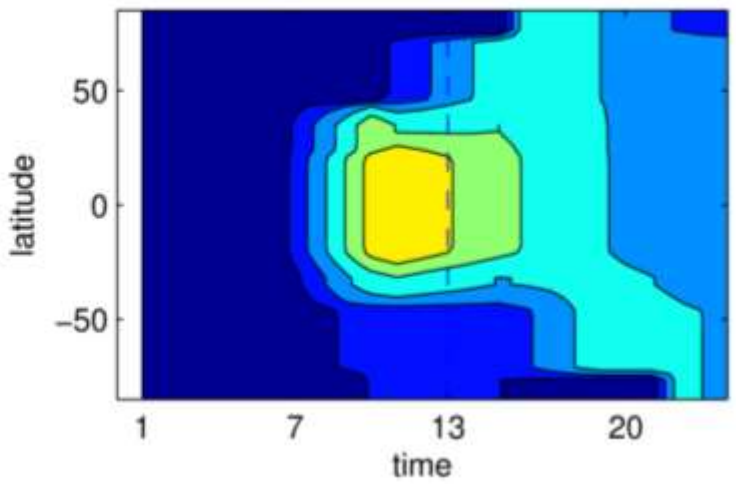

Ultra Trace Chemistry Lab at DRI

Continuous Flow Analysis of Ice Cores using CFA-BC-TE-GAS

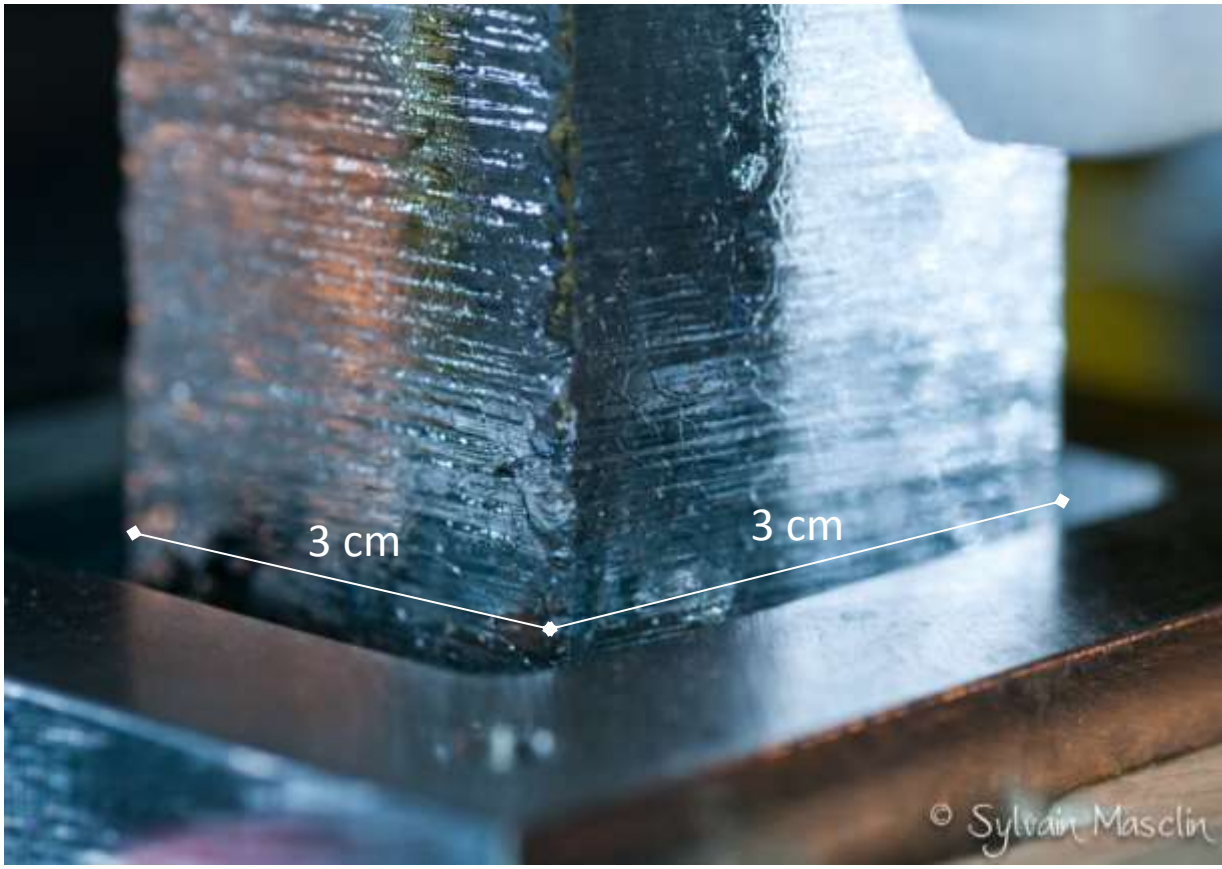

By using black carbon measurements and many other parameters from new, real-time, high-resolution measurement techniques for annual layer dating, we could develop a history of sulfate deposition for Antarctica for the past 2,500 years.

slide provided by Michael Sigl

Volcanic ice-core synchronization

Annual sulphur concentrations

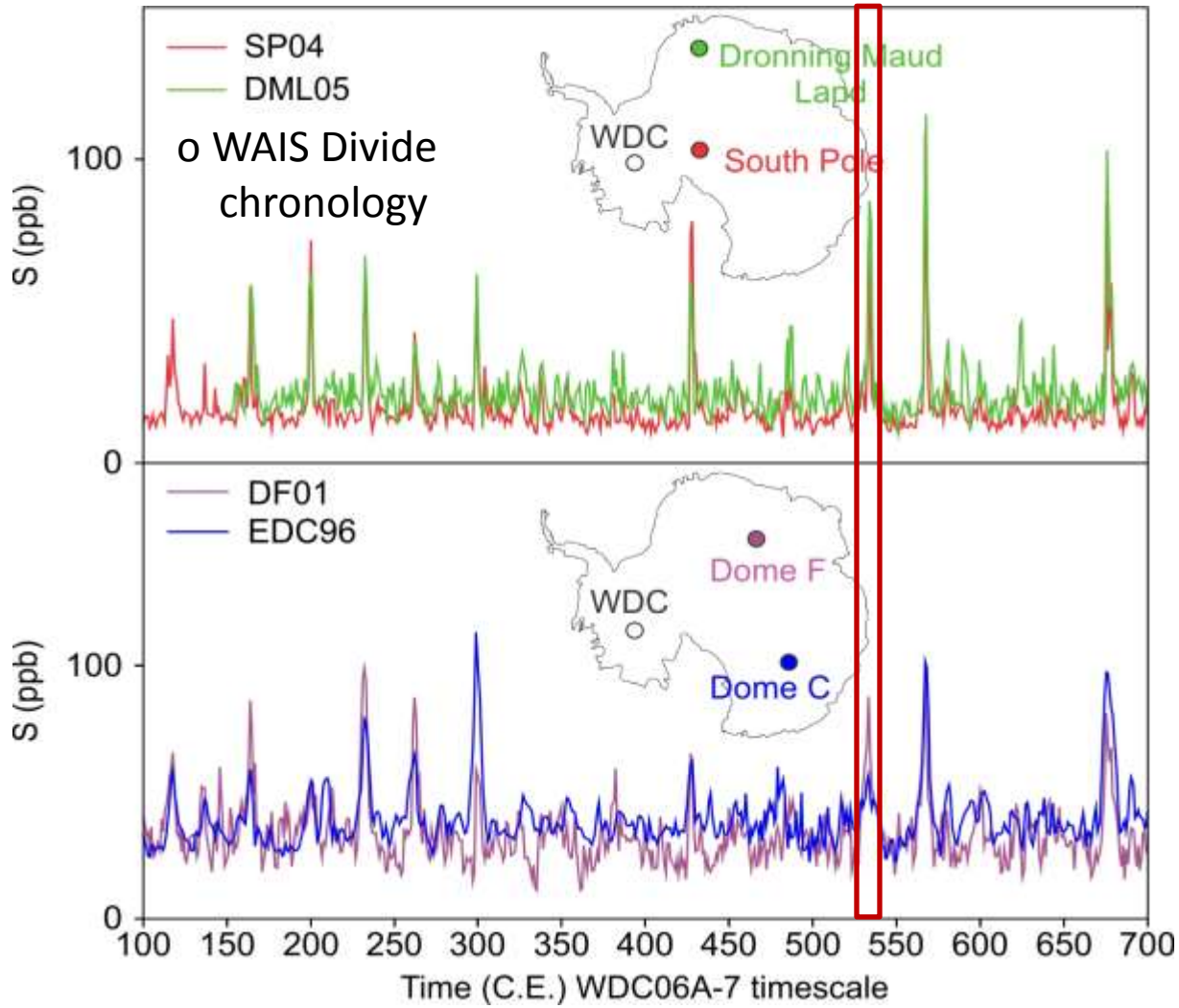

Ice cores

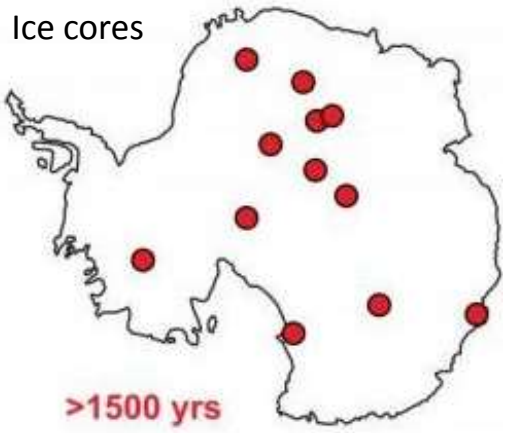

531 UE ice cores vs 45Mt SO_2 model

r=0.48 b=4.1

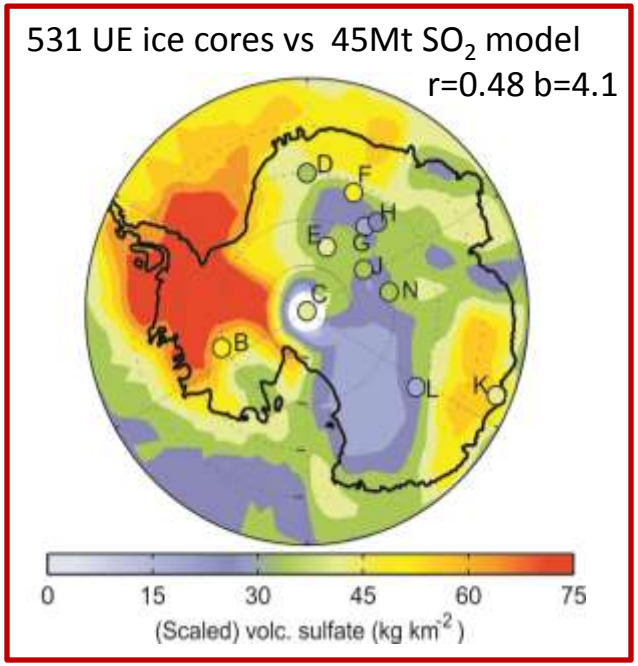

With 12 records covering the past 1,500 years, we can reconstruct robust estimates of sulfate deposition on larger spatial scales.

Sigl et al. 2014, Nature Clim. Change

Stratospheric aerosol loading in the Southern Hemisphere

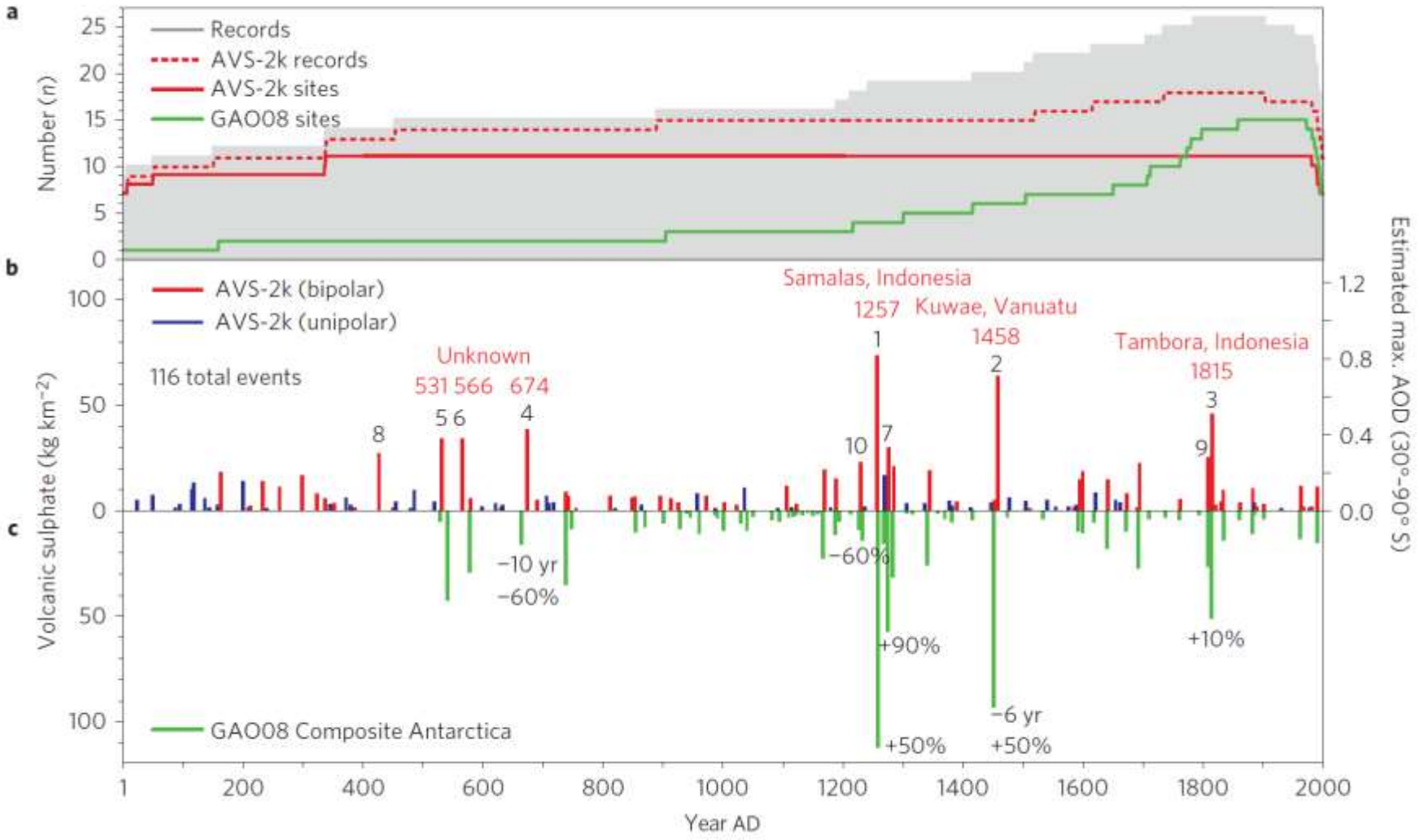

A comparison with Gao et al (2008) based on earlier ice core compilations shows that during the past 500yr, when both of the reconstructions are based on a similar sample size, the values agree very well; whereas the differences prior to 1500 AD are larger in both magnitude and timing.

Sigl et al. 2014, Nature Clim. Change

New bipolar ice core chronologies

1

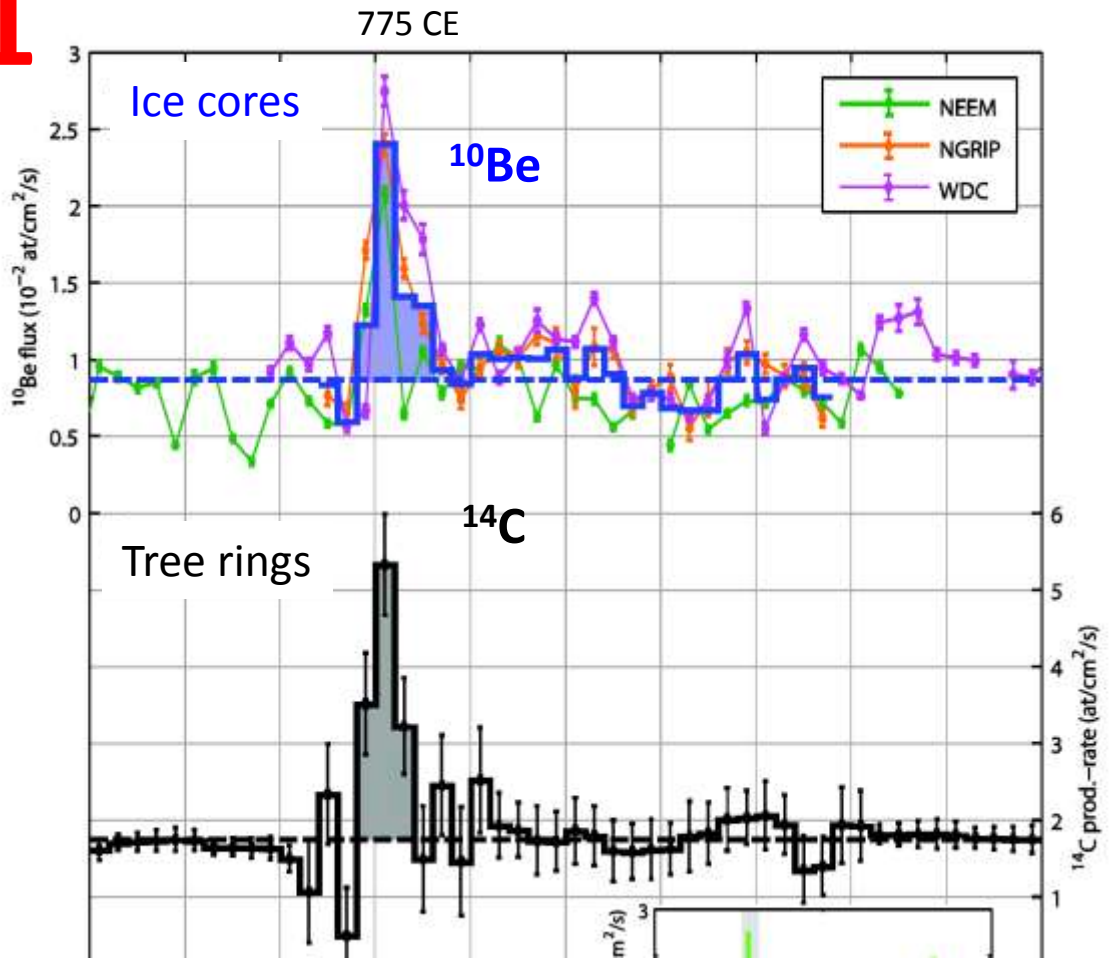

Mekhaldi et al. in review

2

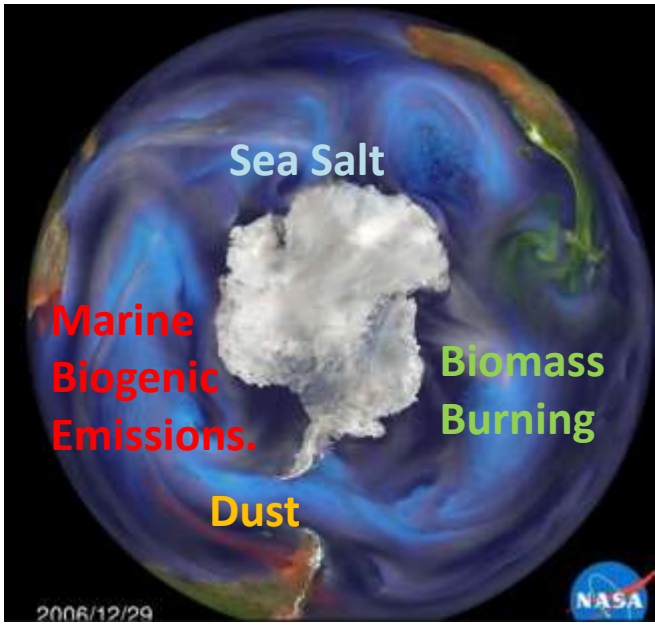

3

"StratiCounter"

Revision of ice core chronologies in Greenland and Antarctica up to 10 years during 1st Millennium by: **1)** using a **fixed age marker in 775 CE**, **2)** constrained annual layer dating using **multi-parameter aerosol records**, **3)** applying an **objective algorithm**.

slide provided by Michael Sigl

Post-volcanic cooling during the past 2,500 years

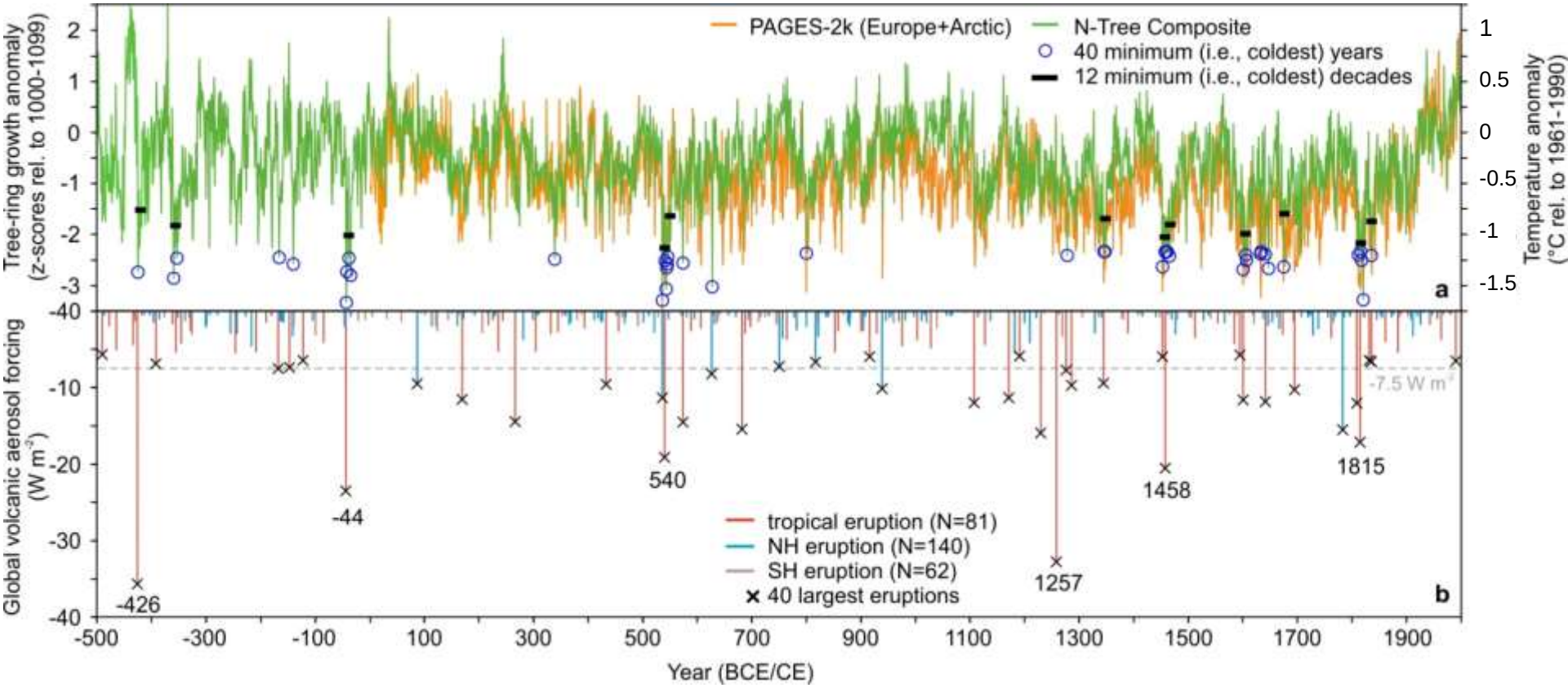

Sigl et al. 2015 Nature

Last Millennium 1 ka

Reconstructed solar forcing

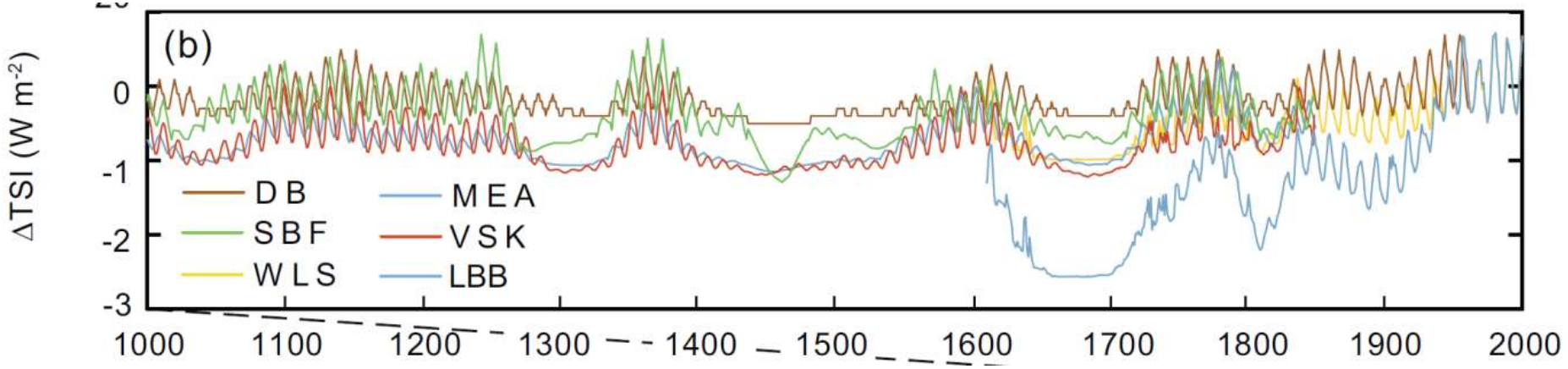

Maunder Minimum
1645-1715

Solar activity proxy: sunspots and ^{10}Be

All reconstructions have been used for PIMP3/CMIP5 simulations expect Lean et al 1995b (LBB), which has been widely used before that.

IPCC Chapter 5 (2013)

Temporal variations of the solar insolation

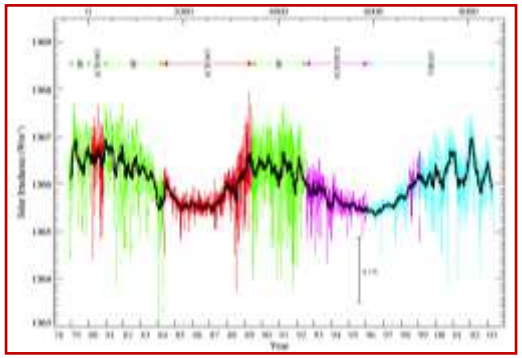

- The solar constant is not constant
- ~27-day rotation cycle of the sun
- ~11-year sunspot cycle
- Centennial scales
- Milankowich (1941): influence of the earth orbit parameter on the ice age cycles was confirmed by Hays et al. (1976).

The 11-year solar cycle

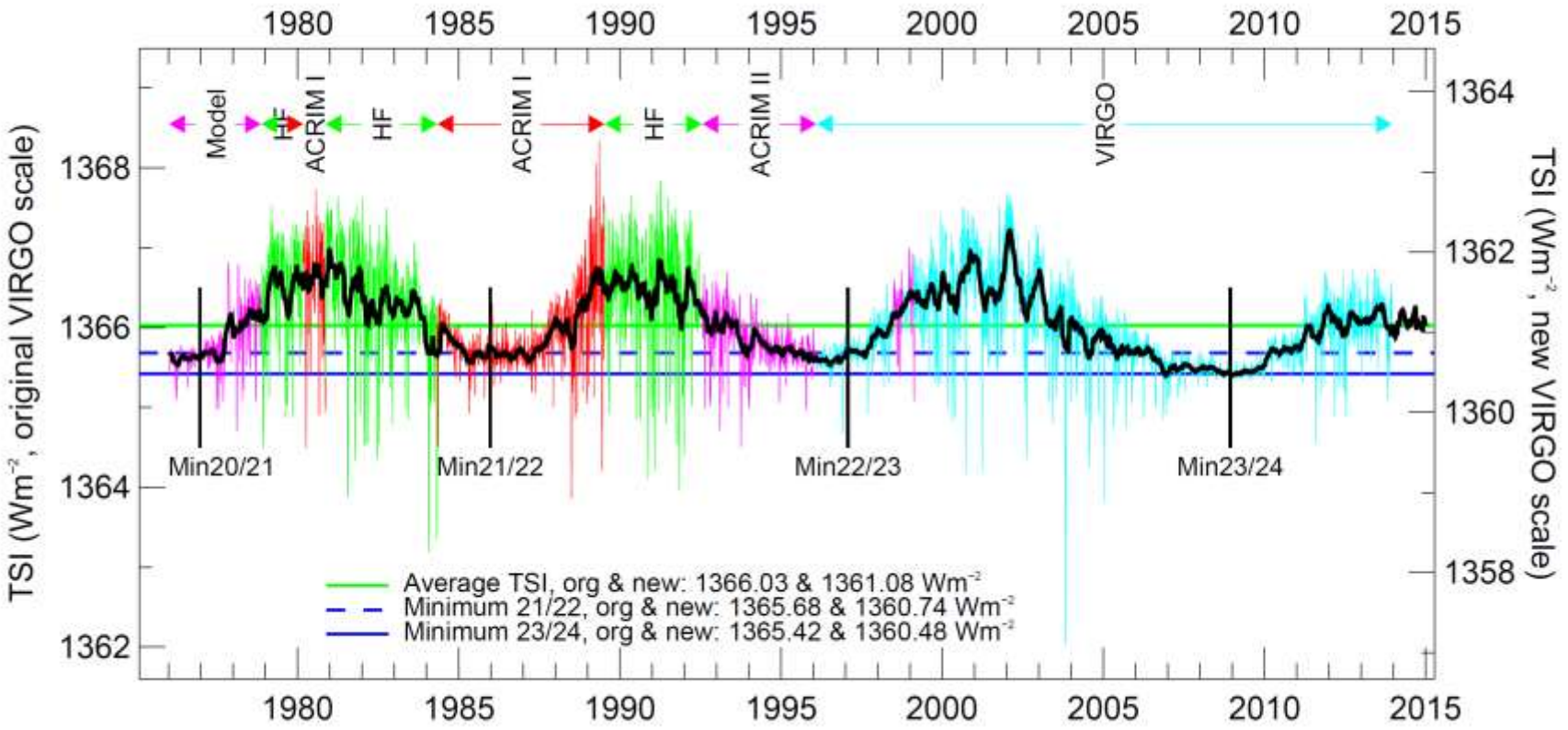

http://www.pmodwrc.ch/pmod.php?topic=tsi/composite/SolarConstant

pmod wrc

Physikalisch-Meteorologisches Observatorium Davos
World Radiation Center

Note new TSI value of ~1361 W/m^2

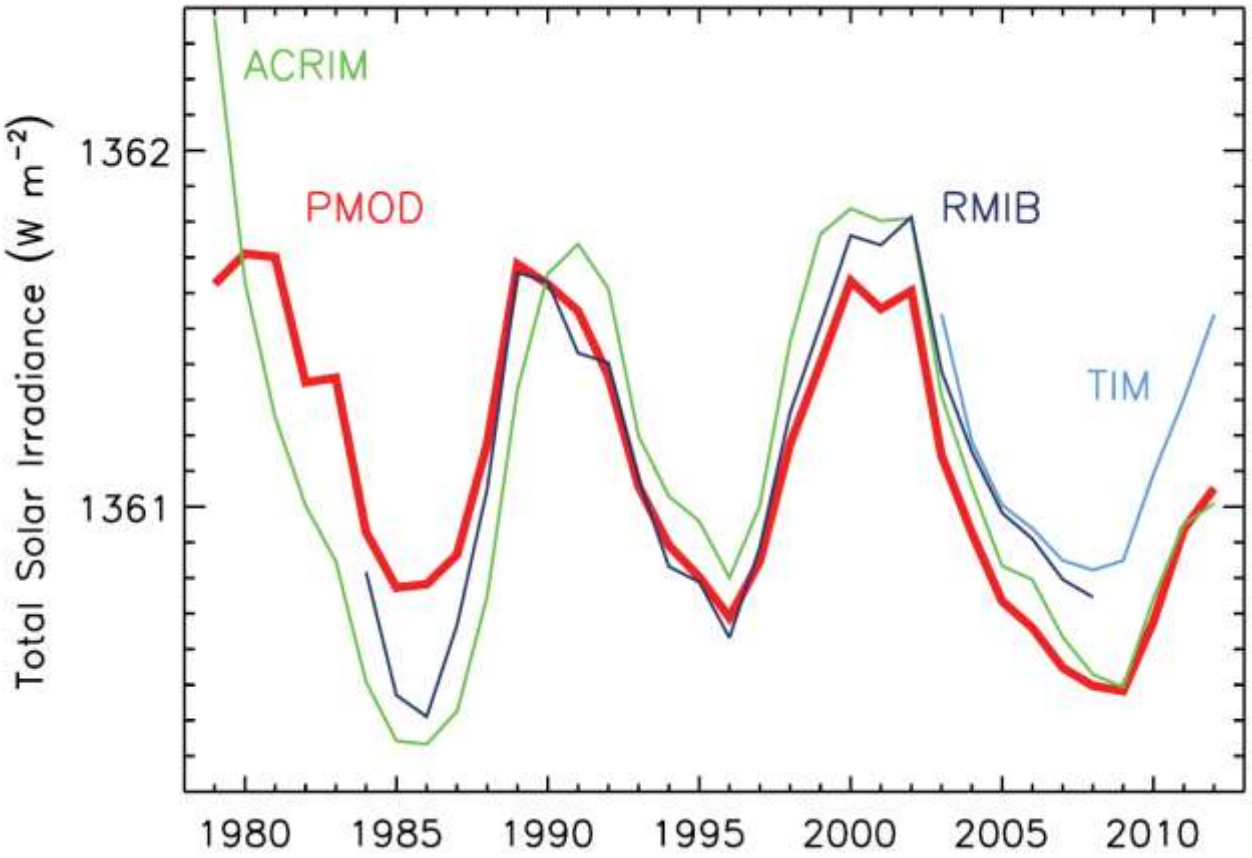

ACRIM: Active Cavity Radiometer Irradiance Monitor
TIM: Total Irradiance Monitor
RMIB: Royal Meteorological Institute of Belgium
PMOD: Physikalisch Meteorologisches Observatorium Davos

Kopp and Lean (2011)
taken from IPCC 2013 Chapter 8

TSI: Total Solar Irradiance

Historical reconstructions of TSI

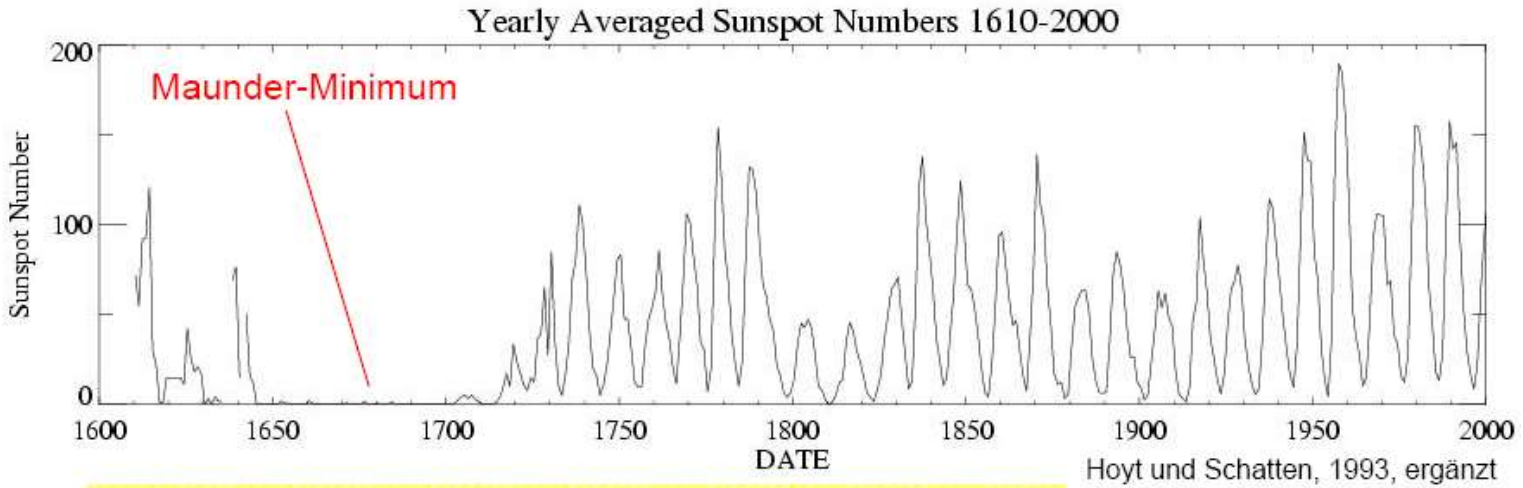

TSI-Zunahme von 1600 bis heute: 2,8 Wm^{-2} (0,2 %) (Lean, 2000)

-Reconstructions are based on physical modeling of the evolution of solar surface magnetic flux...
-All reconstructions rely on indirect proxies that inherently do not give consistent results.
-Large discrepancies among the models.

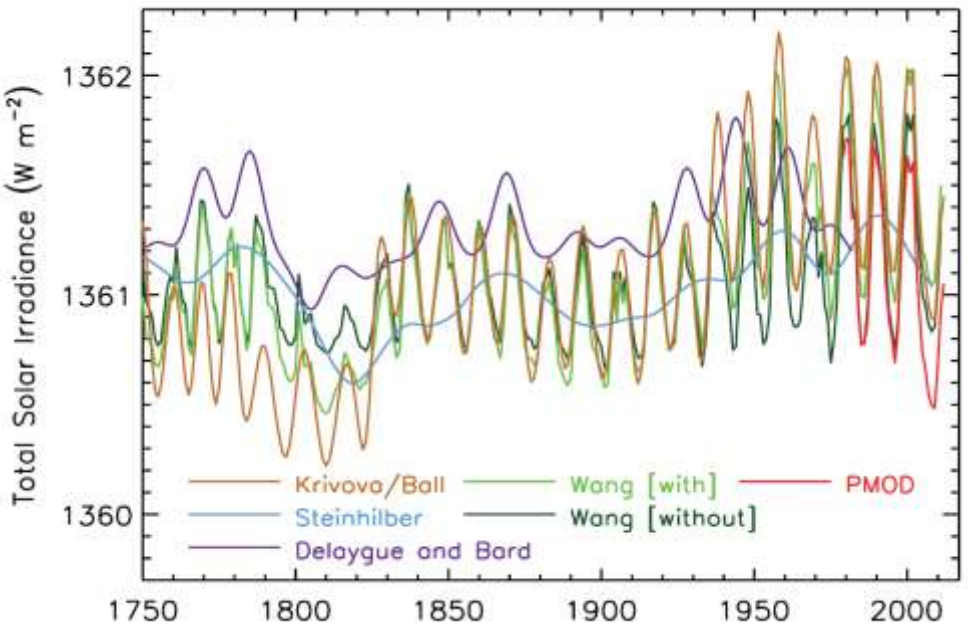

Chapter 8 IPCC (2013)

TSI: Total Solar Irradiance

Orbital Forcing

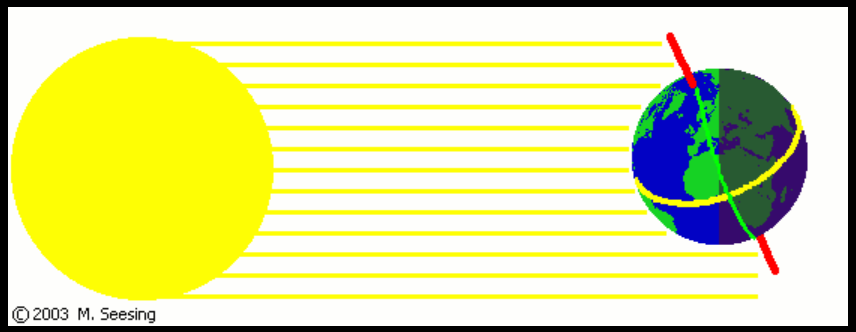

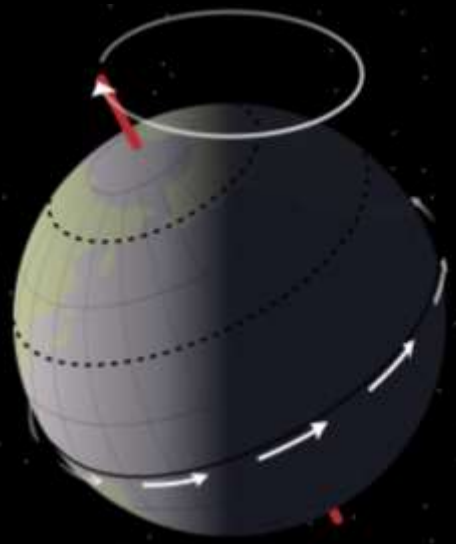

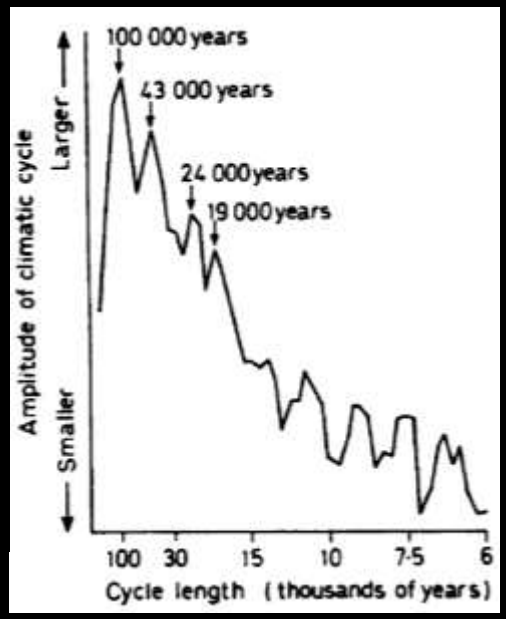

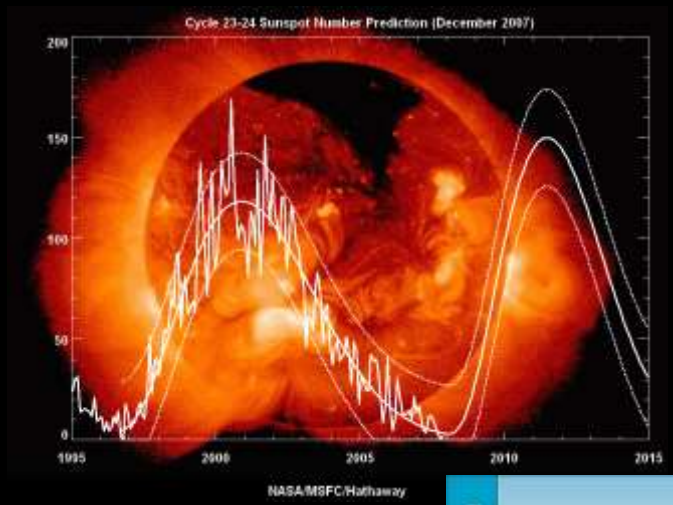

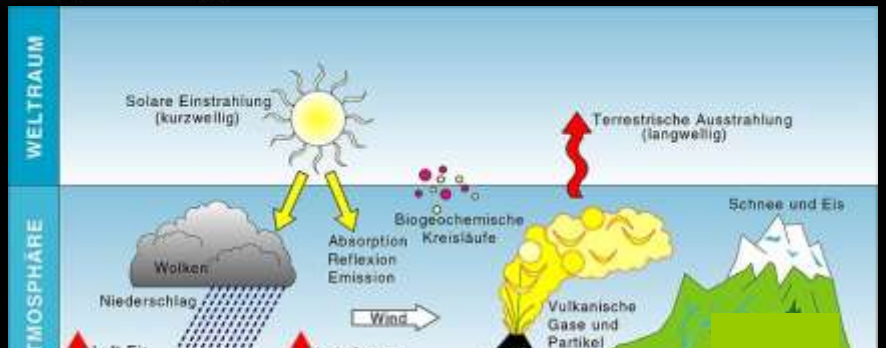

External climate factors

Orbital parameters: 1. Eccentricity

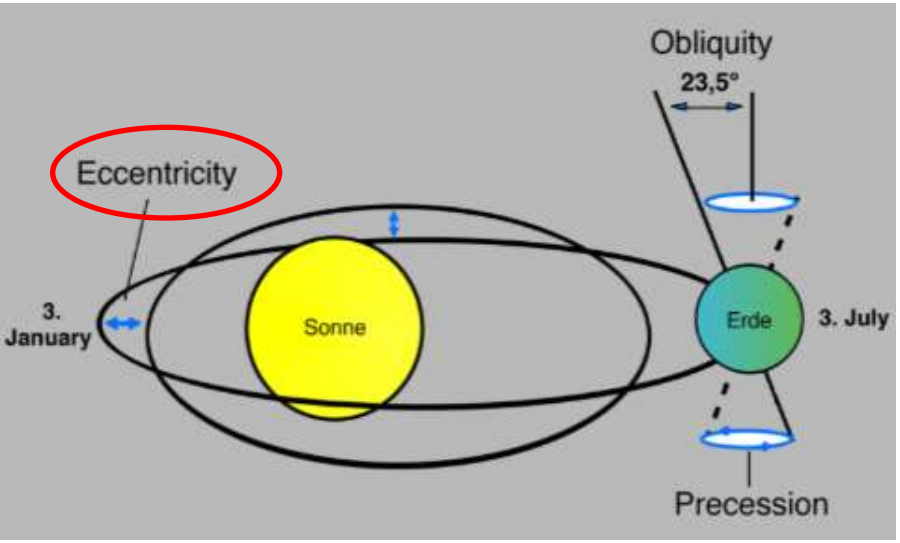

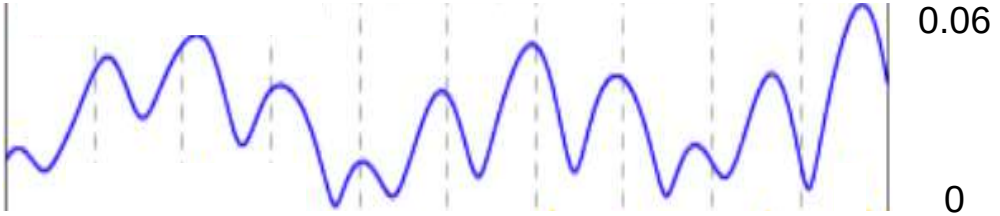

100,000 years, 400,000 years

Time in 1,000 yrs before today 0 200 400 600 800 1,000

External climate factors

Orbital parameters: 2. Obliquity of earth's axis

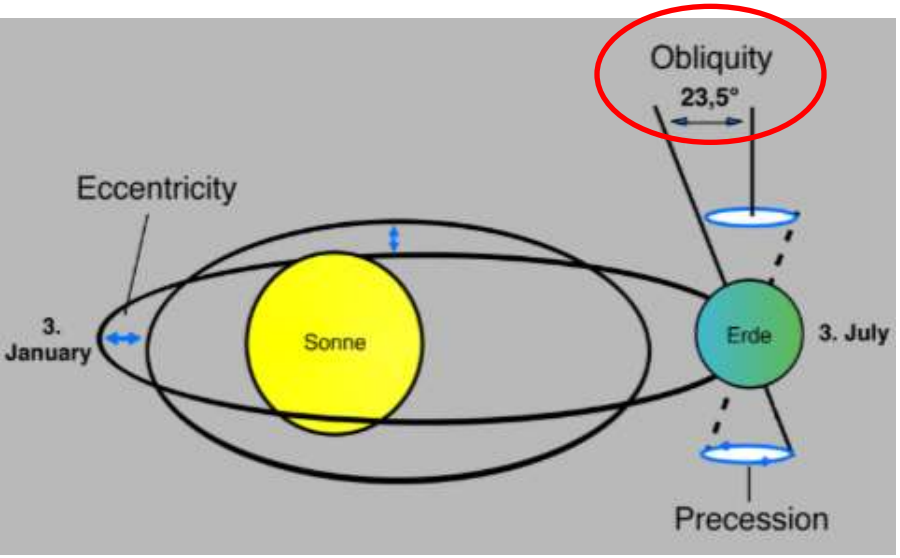

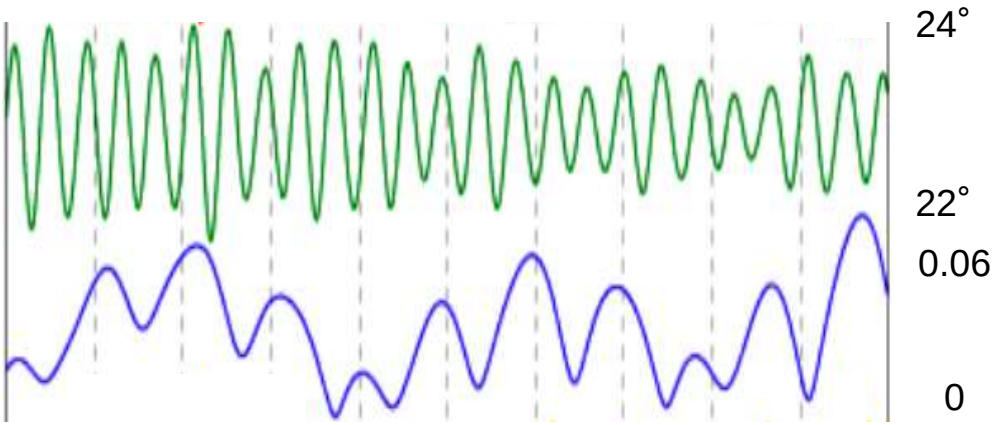

41,000 years

Time in 1,000 yrs before today 0 200 400 600 800 1,000

External climate factors

Orbital parameters: 3. Precession

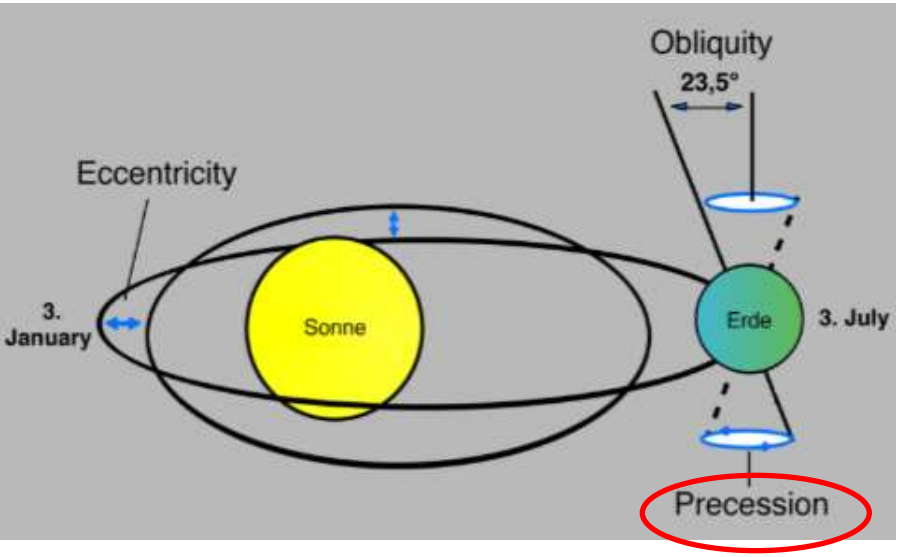

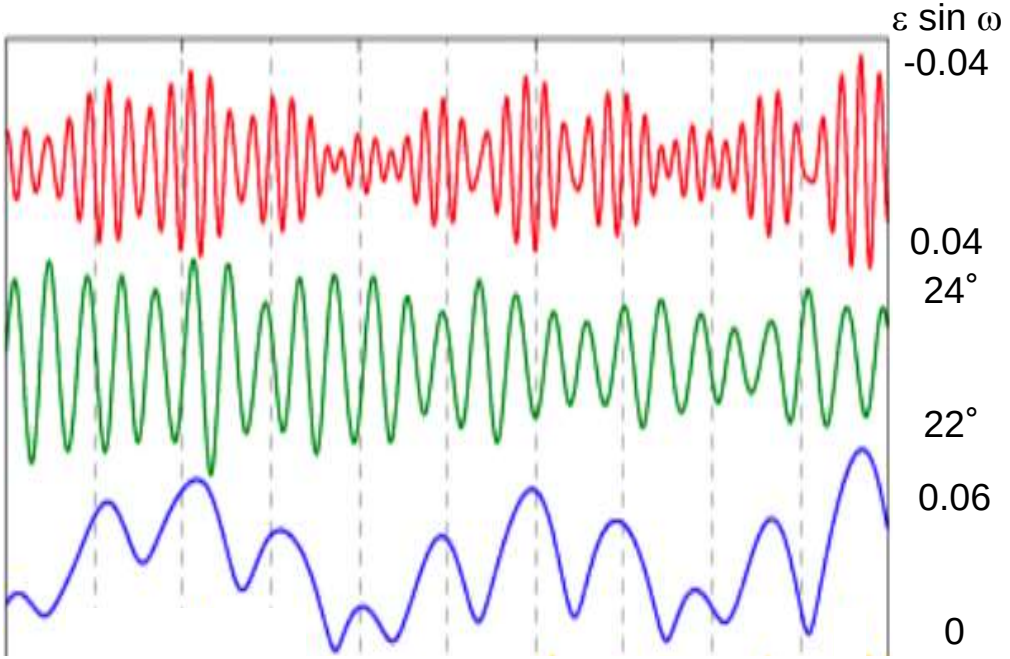

21,000 years

Time in 1,000 yrs before today 0 200 400 600 800 1,000

External climate factors

Orbital parameters

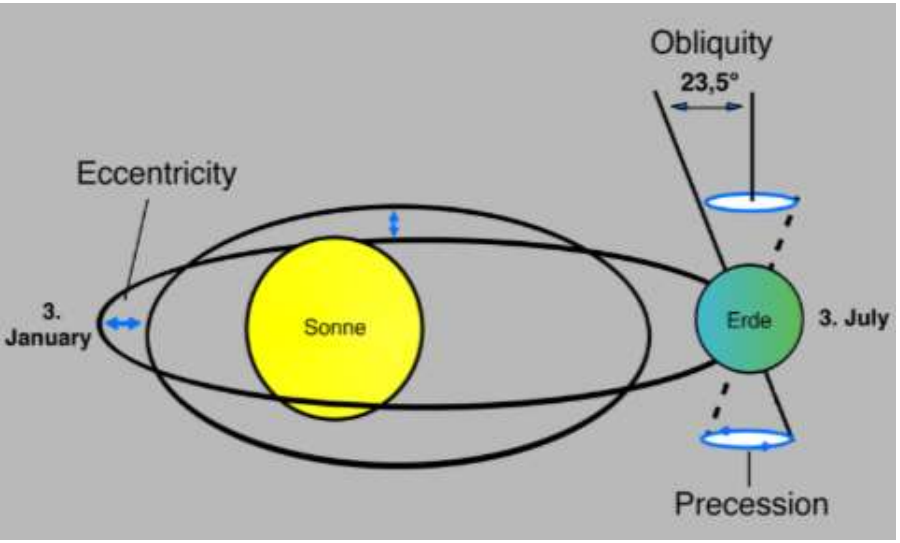

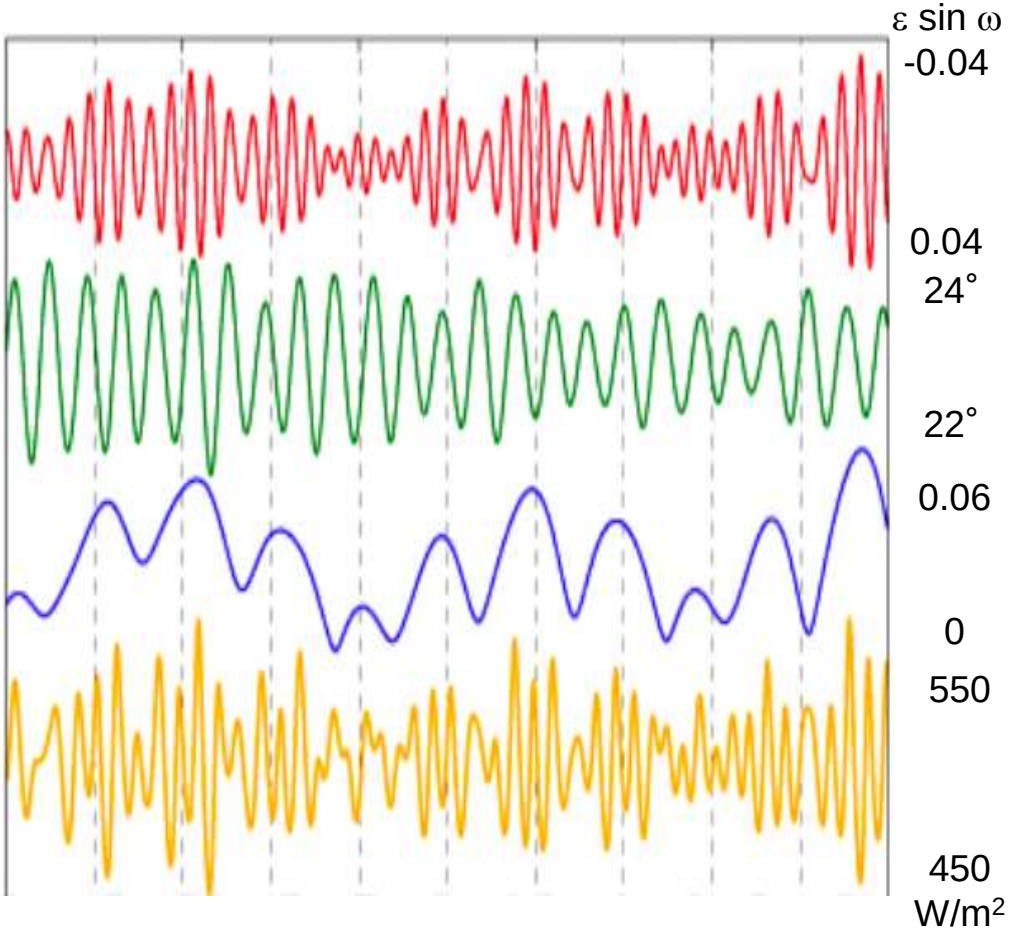

Solar radiation in NH summer at 65° N

Time in 1,000 years before today 0 200 400 600 800 1,000

Milankovitch theory

orbital pacemaker for ice ages

65° N summer insolation

Eemian interglacial

W m^{-2}

550
500
450
400

-200 -150 -100 -50 0 50 100 150 200

future time kyr BP past

Last glacial maximum

… next ice age???

IPCC (2007)

- "The Milankovitch, or 'orbital' theory of the ice ages is now well developed.
- Ice ages are generally triggered by minima in high-latitude NH summer insolation, enabling winter snowfall to persist through the year and therefore accumulate to build NH glacial ice sheets.
- Similarly, times with especially intense high-latitude NH summer insolation, determined by orbital changes, are thought to trigger rapid deglaciations, associated climate change and sea level rise.
- These orbital forcings determine the pacing of climatic changes, while the large responses appear to be determined by strong feedback processes that amplify the orbital forcing.
- Over multi-millennial time scales, orbital forcing also exerts a major influence on key climate systems such as the Earth's major monsoons, global ocean circulation and the greenhouse gas content of the atmosphere.
- Available evidence indicates that the current warming will not be mitigated by a natural cooling trend towards glacial conditions.
- **Understanding of the Earth's response to orbital forcing indicates that the Earth would not naturally enter another ice age for at least 30,000 years. "**

Past 3.5 Ma – Climate Changes

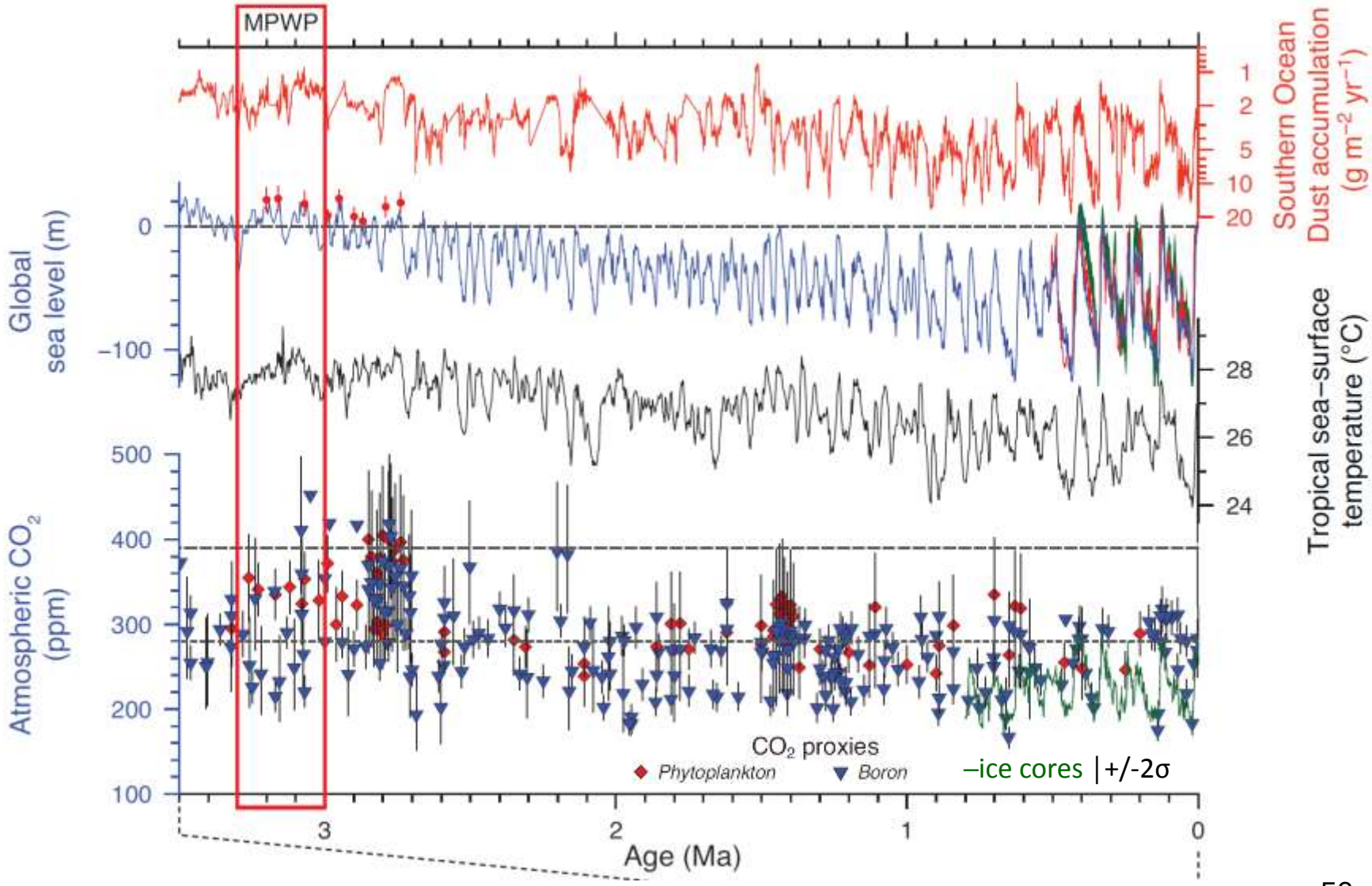

MPWP: Mid Pliocene Warm Period (3.3 to 3 Ma)

Past 65 Ma - Atmospheric CO_2

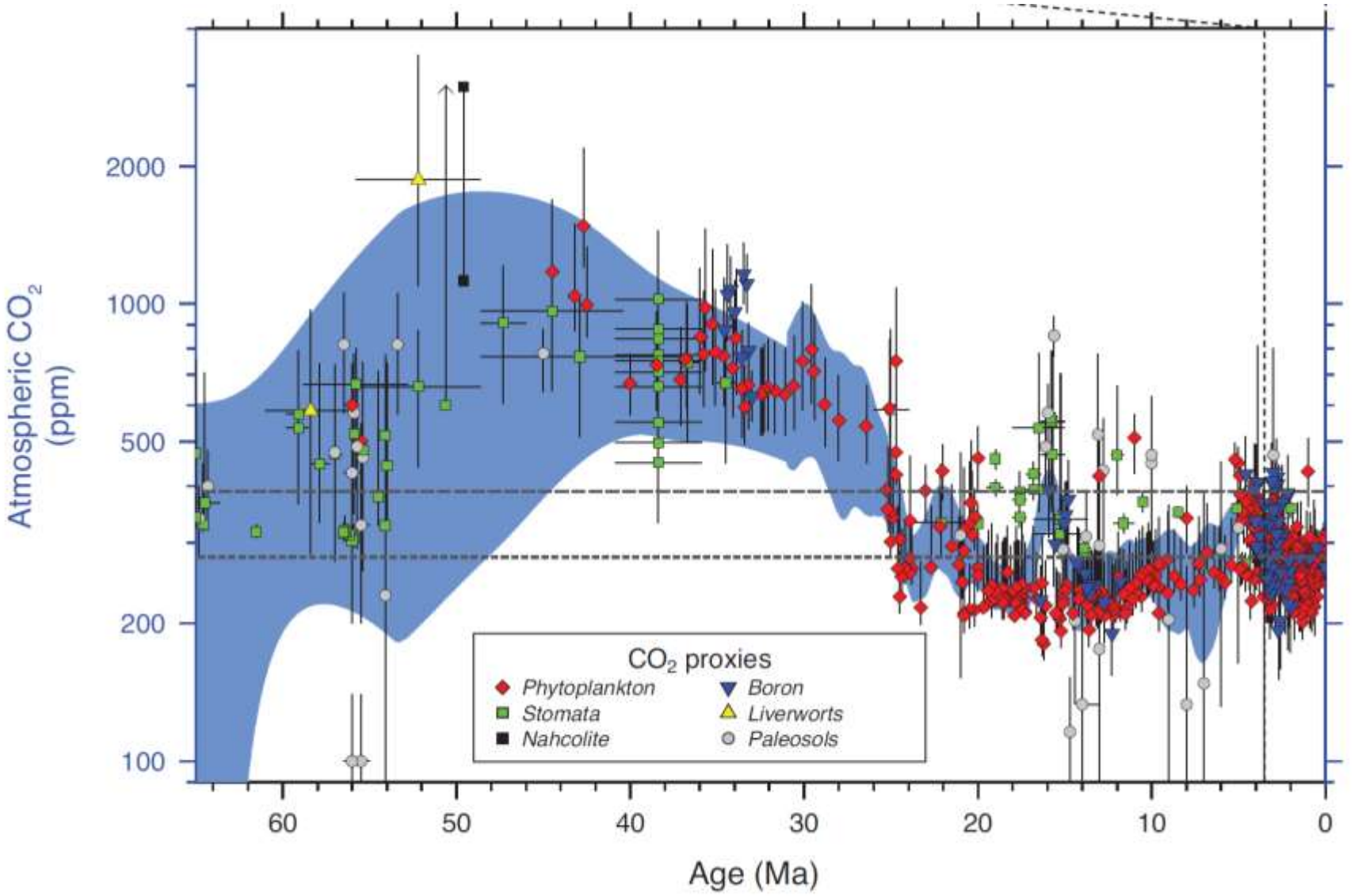

+/- 1σ uncertainty

|+/- 2σ

Earth System Responses and Feedbacks *(Section 5.3)*

Past 800 ka

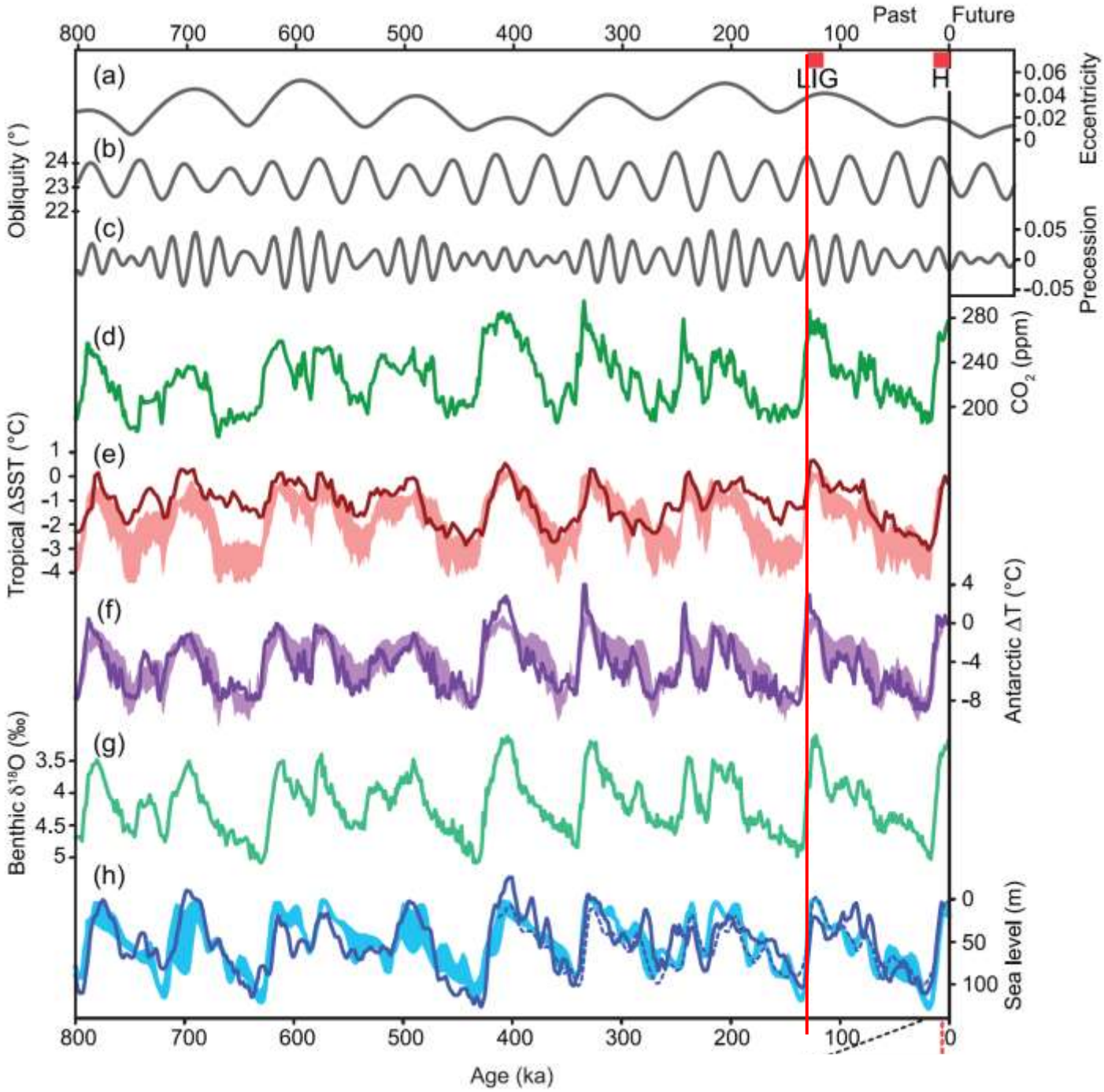

LIG: Last Interglacial
H: Holocene

Box 5.2 | Climate-Ice Sheet Interactions

Ice sheets have played an essential role in the Earth's climate history (see Sections 5.3, 5.6 and 5.7). They interact with the atmosphere, the ocean–sea ice system, the lithosphere and the surrounding vegetation (see Box 5.2, Figure 1). They serve as nonlinear filters and integrators of climate effects caused by orbital and GHG forcings (Ganopolski and Calov, 2011), while at the same time affecting the global climate system on a variety of time scales (see Section 5.7).

Ice sheets form when annual snow accumulation exceeds melting. Growing ice sheets expand on previously vegetated areas, thus leading to an increase of surface albedo, further cooling and an increase in net surface mass balance. As ice sheets grow in height and area, surface temperatures drop further as a result of the lapse-rate effect, but also snow accumulation decreases because colder air holds less moisture (inlay in Box 5.2, Figure 1). This so-called elevation-desert effect (Oerlemans, 1980) is an important negative feedback for ice sheets which limits their growth. Higher elevation ice sheets can be associated with enhanced calving at their margins, because the ice flow will be accelerated directly by increased surface slopes and indirectly by lubrication at the base of the ice sheet. Calving, grounding line processes, basal lubrication and other forms of thermo-mechanical coupling may have played important roles in accelerating glacial terminations following phases of relatively slow ice sheet growth, hence contributing to the temporal saw-tooth structure of the recent glacial–interglacial cycles (Figure 5.3).

Large glacial ice sheets also deflect the path of the extratropical NH westerly winds (Cook and Held, 1988), generating anticyclonic circulation anomalies (Box 5.2, Figure 1), which tend to warm the western side of the ice sheet and cool the remainder (e.g., Roe and Lindzen, 2001). Furthermore, the orographic effects of ice sheets lead to reorganizations of the global atmosphere circulation by changing the major stationary wave patterns (e.g., Abe-Ouchi et al., 2007; Yin et al., 2008) and trade wind systems (Timmermann et al., 2004). This allows for a fast transmission of ice sheet signals to remote regions.

The enormous weight of ice sheets depresses the underlying bedrocks causing a drop in ice sheet height and a surface warming as a result of the lapse-rate effect. The lithospheric adjustment has been shown to play an important role in modulating the ice sheet response to orbital forcing (Birchfield et al., 1981; van den Berg et al., 2008). The presence of terrestrial sedimentary materials (regolith) on top of the unweathered bedrock affects the friction at the base of an ice sheet, and may further alter the response of continental ice sheets to external forcings, with impacts on the dominant periodicities of glacial cycles (Clark and Pollard, 1998).

An area of very active research is the interaction between ice sheets, ice shelves and the ocean (see Sections 4.4, 13.4.3 and 13.4.4). The mass balance of marine ice sheets is strongly determined by ocean temperatures (Joughin and Alley, 2011). Advection of warmer waters below ice shelves can cause ice shelf instabilities, reduced buttressing, accelerated ice stream flow (De Angelis and Skvarca, 2003) and grounding line retreat in regions with retrograde bedrock slopes (Schoof, 2012), such as West Antarctica. On orbital and millennial time scales such processes may have played an essential role in driving ice volume changes of the West Antarctic ice sheet (Pollard and DeConto, 2009) and the Laurentide ice sheet (Alvarez-Solas et al., 2010). Massive freshwater release from retreating ice sheets, can feed back to the climate system by altering sea level, oceanic deep convection, ocean circulation, heat transport, sea ice and the global atmospheric circulation (Sections 5.6.3 and 5.7).

Whereas the initial response of ice sheets to external forcings can be quite fast, involving for instance ice shelf processes and outlet glaciers (10 to 10^3 years), their long-term adjustment can take much longer (10^4 to 10^5 years) (see Section 12.5.5.3). As a result, the climate–cryosphere system is not even in full equilibrium with the orbital forcing. This also implies that future anthropogenic radiative perturbations over the next century can determine the evolution of the Greenland (Charbit et al., 2008) and Antarctic ice sheets for centuries and millennia to come with a potential commitment to significant global sea level rise (Section 5.8). *(continued on next page)*

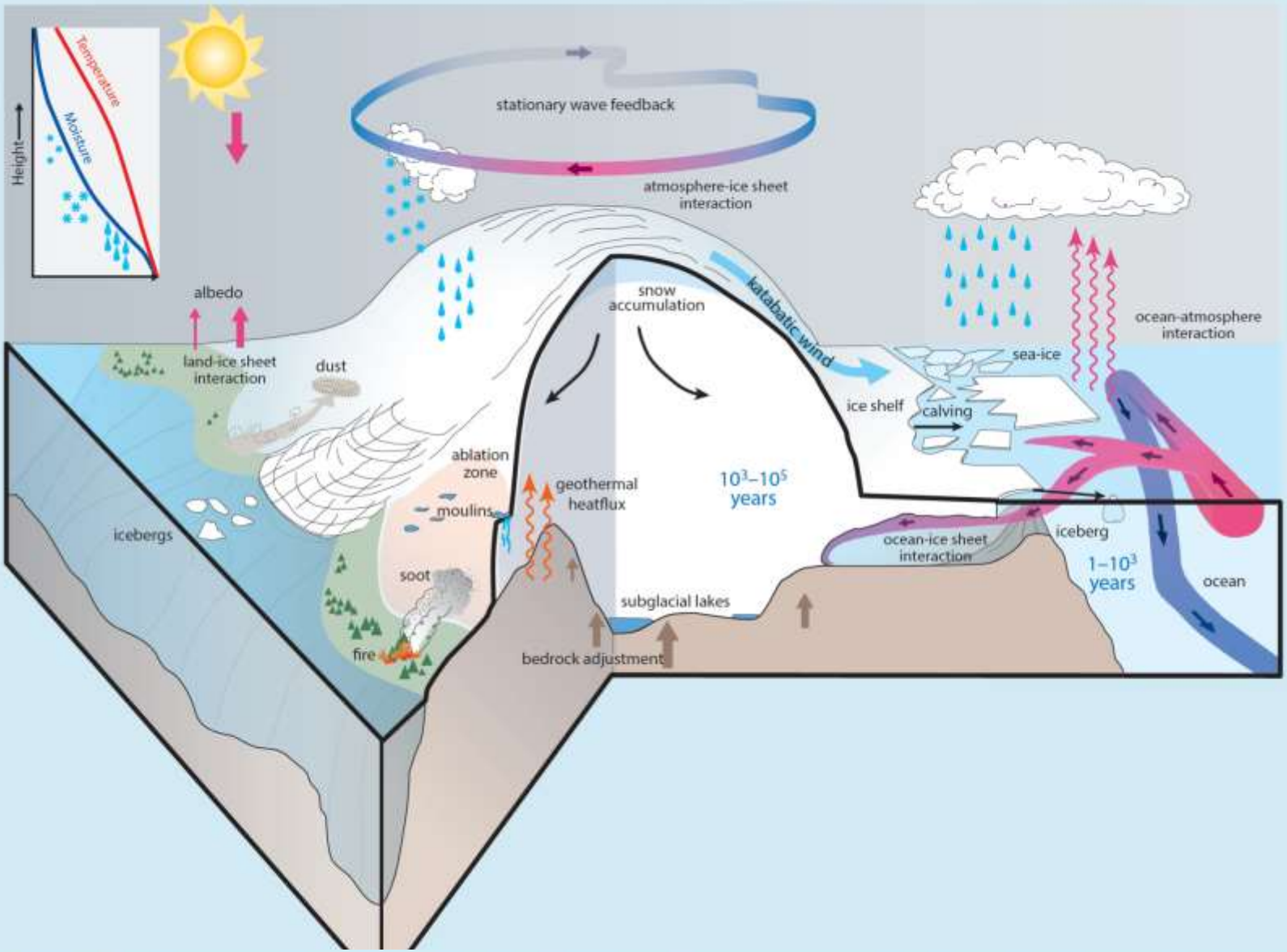

Box 5.2, Figure 1 | Schematic illustration of multiple interactions between ice sheets, solid earth and the climate system which can drive internal variability and affect the coupled ice sheet–climate response to external forcings on time scales of months to millions of years. The inlay figure represents a typical height profile of atmospheric temperature and moisture in the troposphere.

Reconstructions

NH

SH

Global

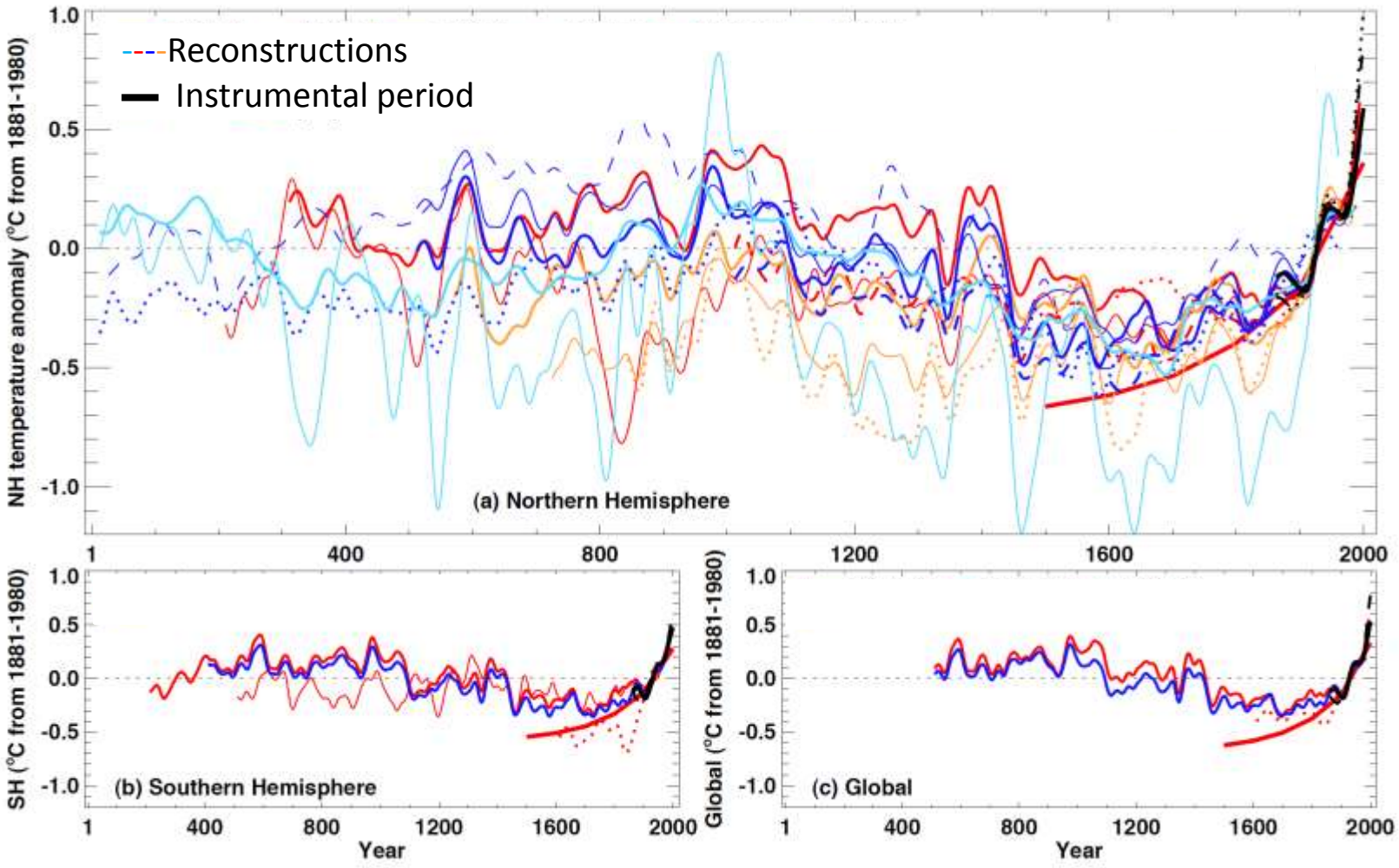

NH surface temperature changes

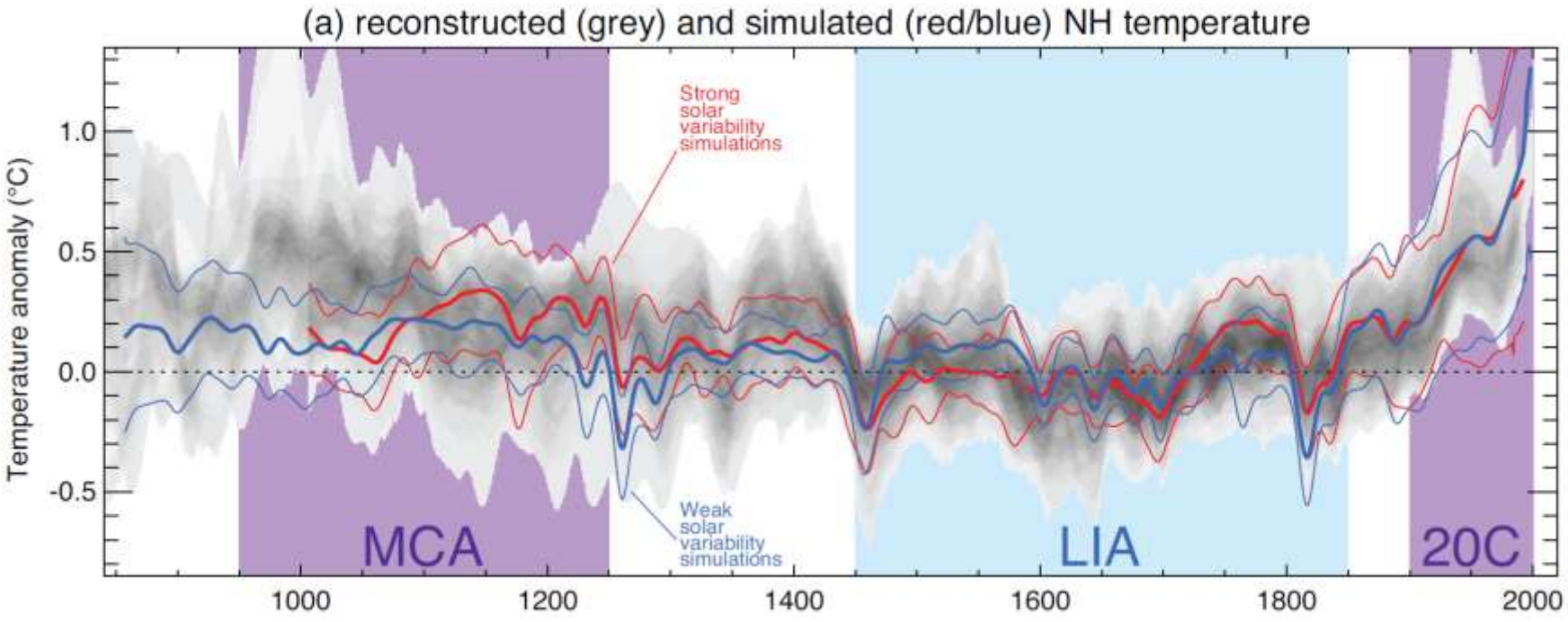

Models:

-Strong solar variability sims

-Weak solar variability sims

▬multi-model mean

– multi-model 90% range

MCA: Medieval Climate Anomaly

LIA: Little Ice Age

20C: 20th Century

IPCC Chapter 5: **Informations from paleoclimate archives**

- Introduction *(Section 5.1)*
- Pre-industrial perspective on radiative forcing factors *(Section 5.2)*
- Earth System Responses and Feedbacks *(Section 5.3)*
- Executive summary *(Ch. 5)*

Masson-Delmotte, V., et al., 2013: Information from Paleoclimate Archives. In: Climate Change 2013: The Physical Science Basis. Contribution of Working Group I to the Fifth Assessment Report of the Intergovernmental Panel on Climate Change. Cambridge University Press.

NH surface temperature changes

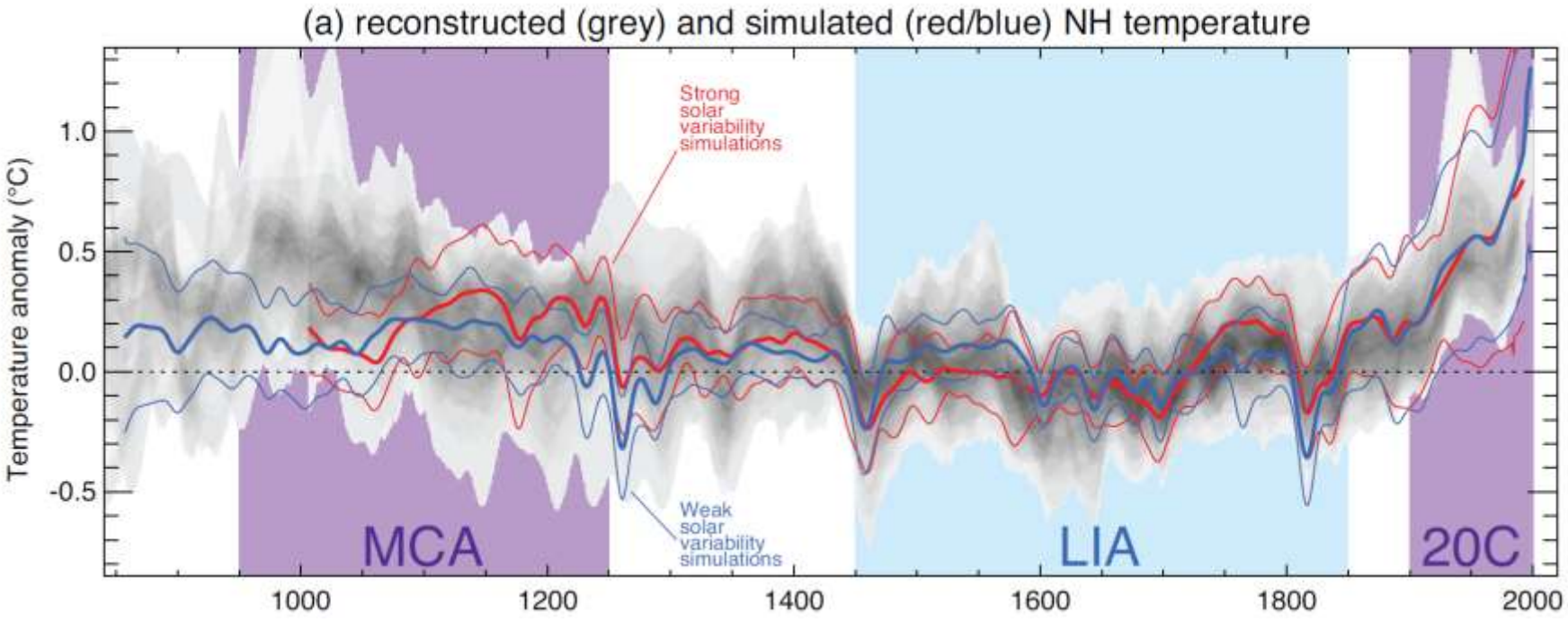

Models:
-Strong solar variability sims
-Weak solar variability sims
▬multi-model mean
– multi-model 90% range

MCA: Medieval Climate Anomaly
LIA: Little Ice Age
20C: 20th Century

Volcanic vs solar forcing and climate response

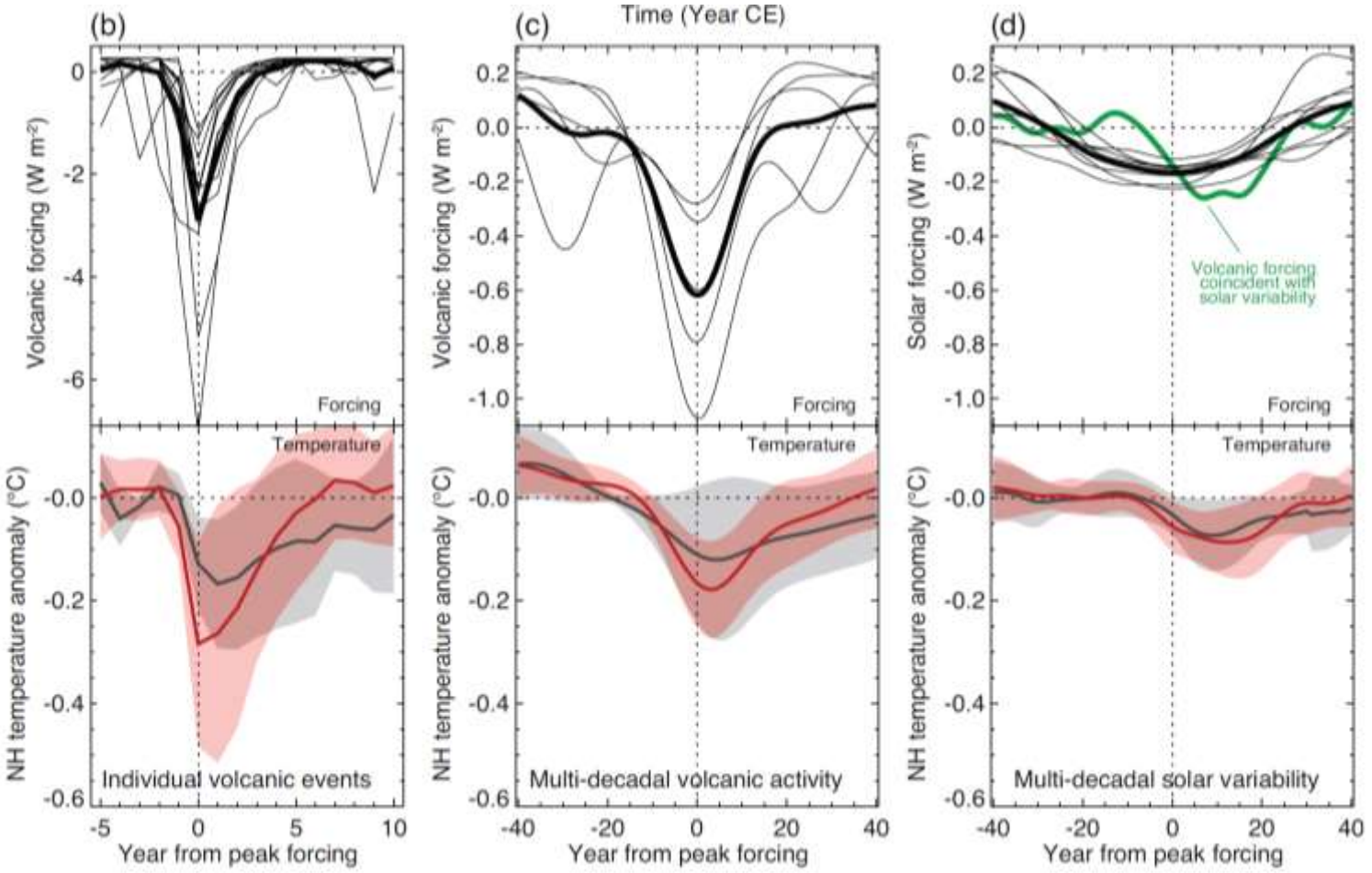

Cold-Warm Period: NH temp

MCA-LIA and 20C-LIA

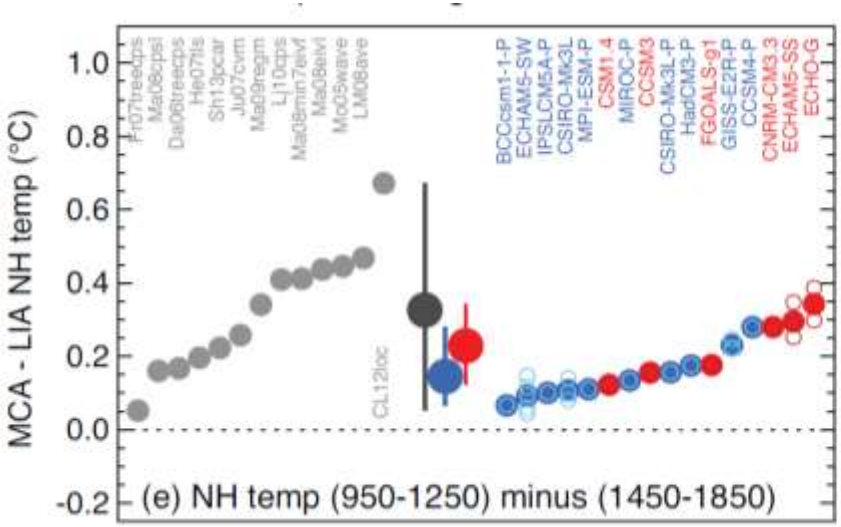

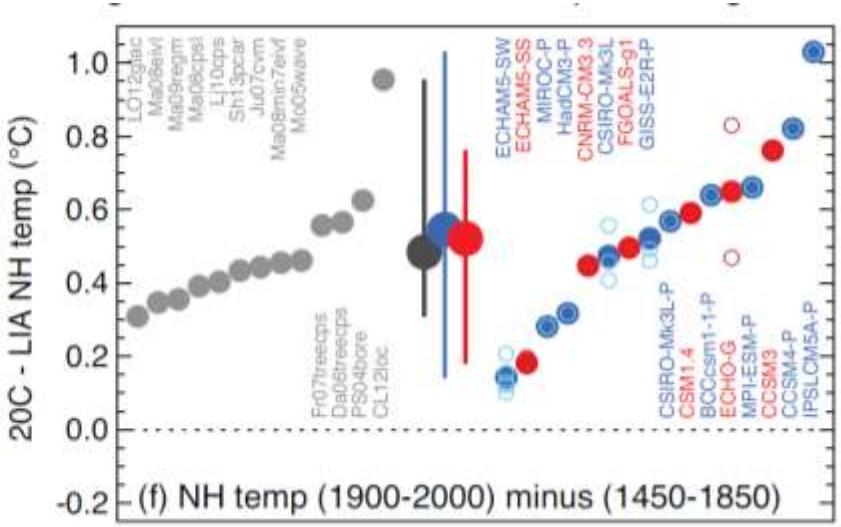

MCA: Medieval Climate Anomaly
LIA: Little Ice Age
20C: 20th Century

Executive Summary

Excecutive Summary -I

Greenhouse-Gas Variations and Past Climate Responses

- **It is a fact that present-day (2011) concentrations of the atmospheric greenhouse gases (GHGs) carbon dioxide (CO_2), methane (CH_4) and nitrous oxide (N_2O) exceed the range of concentrations recorded in ice cores during the past 800,000 years.**
- **With very high confidence, the current rates of CO_2, CH_4 and N_2O rise in atmospheric concentrations and the associated radiative forcing are unprecedented with respect to the highest resolution ice core records of the last 22,000 years.**
- **There is high confidence that changes in atmospheric CO_2 concentration play an important role in glacial–interglacial cycles.** Although the primary driver of glacial–interglacial cycles lies in the seasonal and latitudinal distribution of incoming solar energy driven by changes in the geometry of the Earth's orbit around the Sun ("orbital forcing"), reconstructions and simulations together show that the full magnitude of glacial–interglacial temperature and ice volume changes cannot be explained without accounting for changes in atmospheric CO_2 content and the associated climate feedbacks.

Excecutive Summary - II

With medium confidence, global mean surface temperature was significantly above pre-industrial levels during several past periods characterised by high atmospheric CO2 concentrations.

- During the mid-Pliocene (3.3 to 3.0 million years ago), atmospheric CO2 concentrations between 350 ppm and 450 ppm (medium confidence) occurred when global mean surface temperatures were 1.9° C to 3.6° C (medium confidence) higher than for pre-industrial climate.
- During the Early Eocene (52 to 48 million years ago), atmospheric CO2 concentrations exceeded ~1000 ppm (medium confidence) when global mean surface temperatures were 9° C to 14° C (medium confidence) higher than for pre-industrial conditions.
- **New temperature reconstructions and simulations of the warmest millennia of the last interglacial period (129,000 to 116,000 years ago) show with medium confidence that global mean annual surface temperatures were never more than 2° C higher than pre-industrial.**

Excecutive Summary - III

- **There is high confidence that annual mean surface warming since the 20th century has reversed long-term cooling trends of the past 5000 years in mid-to-high latitudes of the Northern Hemisphere (NH).** New continental- and hemispheric-scale annual surface temperature reconstructions reveal multi-millennial cooling trends throughout the past 5000 years. The last mid-to-high latitude cooling trend persisted until the 19th century, and can be attributed with high confidence to orbital forcing, according to climate model simulations. {5.5.1}